An Overview on Medium Voltage Grid Integration of Ultra-Fast Charging Stations: Current Status and Future Trends

ADNAN AHMAD [1] (Student Member, IEEE), ZIAN QIN [1] (Senior Member, IEEE),
THIWANKA WIJEKOON [2] (Senior Member, IEEE), AND PAVOL BAUER[1] (Senior Member, IEEE)

[1]Department of Electrical Sustainable Energy, Delft University of Technology, 2628 CD Delft, Netherlands
[2]Huawei's Nuremberg Research Center, 90449 Nürnberg, Germany

CORRESPONDING AUTHOR: ZIAN QIN (e-mail: z.qin-2@tudelft.nl)

ABSTRACT The emphasis on clean and green technologies to curtail greenhouse gas emissions due to fossil fuel-based economies has originated the shift towards electric mobility. As on-road electric vehicles (EVs) have shown exponential growth over the last decade, so have the charging demands. The provision of charging facilities from the low-voltage network will not only increase the distribution system's complexity and dynamics but will also challenge its operational capabilities, and large-scale upgrades will be required to meet the inevitably increasing charging demands. An ultra-fast (UF) charging infrastructure that replicates the gasoline refueling network is urgently needed to facilitate a seamless transition to EVs and ensure smooth operation. This paper presents a review of state-of-the-art DC fast chargers, the charging infrastructure's current status, motivation, and challenges for medium-voltage (MV) UF charging stations (UFCS). Furthermore, we consider the possible UFCS architectures and suitable power electronics topologies for UF charging applications. To address the peak formation issues in the daily load profile and high operational expenses of UFCSs, integration of renewable energy sources and energy storage systems due to their technological and economic benefits is being considered. The benefits of line frequency transformer (LFT) replacement with a solid-state transformer (SST), SST models, SST-based UF chargers, and MV SST-based UFCS architectures, as well as related MV active front-end and back-end power electronics topologies, are presented. Finally, the application of microgrids' hierarchical control architecture is considered for chargers and system-level control and management of UFCSs.

INDEX TERMS Electric vehicles (EVs), DC fast chargers, ultra-fast charging stations (UFCS), renewable energy sources (RESs), energy storage systems (ESSs), line frequency transformer (LFT), solid state transformer (SST).

I. INTRODUCTION

Reliance on fossil fuels has significantly increased the concentration of greenhouse gases (GHG) in the atmosphere, resulting in global warming and ecological disorders. With increased awareness, carbon dioxide (CO_2) emissions and the continuous rise in the global mean temperature have become central points of growing concern in the international community [1]. In this regard, the adaptation of the Paris agreement by 196 countries in December 2015 is an example of the collaborative efforts to combat climate change [2]. Under the umbrella of this agreement, various organizations have been working on multiple fronts, ranging from reforestation to the induction of renewable and sustainable technologies having minimal GHG emissions. Furthermore, the transportation sector has been identified as one of the most promising areas that can contribute significantly to achieving the net zero-emission (NZE) goal [3], [4]. Even though commercial production of electric vehicles (EVs) began in 1996 and the EV initiative (EVI), a multi-governmental policy forum, was founded in 2010. However, the adoption of the Paris agreement accelerated the transition towards electric mobility (e-mobility), and campaigns such as EV30@30 [5], with the

inspirational aim of achieving a 30% sales share of EVs by 2030, and the global commercial vehicle drive to zero [6], to make zero-emission technologies commercially competitive by 2025, were launched in 2017 and 2020, respectively. In addition, to support low and middle-income countries' shift towards e-mobility, the global environment facility program for global e-mobility is set to be launched before 2022 [7].

Historically, the three major challenges to EV adoption were high purchase prices, range anxiety, and a lack of charging infrastructure [8]. However, the advancements in battery technology, power electronics, and magnetics and the various subsidies and incentives have substantially normalized these challenges. The exponentially increasing number of on-road EVs is primarily aided by numerous government initiatives to make EVs more accessible and affordable to customers. Section II presents the details of some of these economic perks offered by different countries.

In terms of range anxiety, progressions in battery and electric propulsion drive-train technologies have remedied the problem. For instance, the average specific energy of a battery was 110 W-hour per kilogram (Wh/kg) in 2010 [9]. Presently, the specific energy of various lithium-ion (Li-ion) batteries lies between 200 and 250 Wh/kg, and projected to reach 450 Wh/kg till 2030 [10]. Similarly, battery energy density has improved from 310 W-hour per liter (Wh/L) to 580 Wh/L in the recent decade, with the next goal of 1100 Wh/L by by 2030 [11], [12]. Aside from batteries, traction inverters' power density also improved from 10 kilowatts per liter (kW/L) to 30 kW/L and expected to reach 65 kW/L by 2030 [13]. Similarly, inverters' peak efficiency increased from 92% to 96%; wide band-gap technologies such as silicon carbide (SiC) and gallium nitride (GaN) have shown efficiencies up to 99% [14], [15]. Moreover, it is projected that the applications of SiC and GaN in traction inverters will achieve a power density of 65 kW/L [16], and 800 V internal DC-link will achieve up to 40% reduction in volume [17]. Although, the range anxiety and battery cost issues have been significantly resolved with the earlier mentioned developments. However, EVs' range per charge is still limited as compared to gasoline vehicles have an average energy density of 12000 Wh/kg [18], [19].

Even exclusive of battery limitations, the absence of a refueling infrastructure capable of rapidly replenishing an EV's battery, especially during longer trips, still remains a decisive barrier. In countries with emerging numbers of on-road EVs, the drivers demand more flexible and efficient charging infrastructure. For over 10 million EVs, the reported number of installed EV supply equipment (EVSE) was 1.3 million globally till 2020, with only 30% of which were fast chargers. The statistics of public charging infrastructure in EV-concentrated regions are presented in Section II.

Presently, low-voltage (LV) distribution networks power the slow and fast charging facilities. Coupled with the charging rates, another point of concern is the exponential growth in EVs. For the projected number of 40 million on-road EVs by 2050 [20], the provision of charging facilities from the LV network will not only increase the distribution system's complexity and dynamics. However, it will also challenge its operational capabilities, and large-scale upgrades will be required to meet the inevitably increasing charging demands. For this reason, an ultra-fast (UF) charging infrastructure with a dedicated medium-voltage (MV) grid connection is urgently required to replicate the existing gasoline infrastructure.

This article reviews EVs and corresponding EVSEs' current trends, presents the anticipated number of on-road EVs and indicates the exponential increase in the past decade. To facilitate a seamless transition towards EVs, state-of-the-art DC fast chargers have been evaluated and emphasized in grouping several fast chargers to form a UF charging station (UFCS). State-of-the-art DC fast chargers have been evaluated, and the grouping of several fast chargers to form a UFCS has been emphasized. A 350 kW can recharge a 60 kWh battery to more than 90% state of charge (SOC) in 10 minutes. However, such an impulsive charging demand requires the grid to maintain high spinning reserves; therefore, this issue has been addressed with the energy storage systems in UFCSs. A solid-state transformer (SST) poses numerous advantages over conventional line frequency transformers (LFT), especially in AC/DC applications, SST models, SST-based UF chargers, and MV SST-based UFCS architectures have been presented. Section IV elaborates on the motivation, requirements and challenges for MV connected UFCSs.

The rest of the paper is organized as follows: Section II provides an overview of EV trends, initiatives aimed at facilitating a seamless transition towards e-mobility, the evolution of battery technologies, and EVSE global statistics. The working principles of alternating current (AC) and direct current (DC) chargers and most relevant international standards are presented in Section III. The motivation and challenges for UFCSs are addressed in Section IV, and Section V look at the AC and DC common bus architectures of UFCSs, respectively. Moreover, the benefits of replacing a line-frequency transformer (LFT) with a solid-state transformer (SST) and SST-based possible configurations have also been explained in Section V. In Section VI, the significance of renewable energy sources (RESs) and energy storage systems (ESSs) integration, as well as their impacts on peak demand and operational expenses of UFCSs, have been discussed. Section VII discusses the future trends and suggestions proposed in the literature regarding EVs and EVSEs, SST, and SST-based integration of UFCSs with MV-grid. Section VIII presents a review of the AC/DC and DC/DC power electronics converters that have been extensively studied for EV charging applications. Moreover, the potential MV AC/DC and DC/DC that can be used for UFCS MV-grid integration have been presented in Section VIII. Section IX accesses hierarchical control structures for dynamic response and ancillary grid services such as power system frequency and voltage regulation, chargers, UFCS-level control, energy management
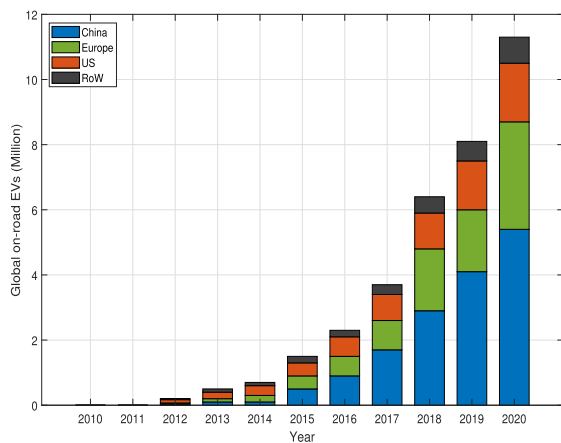
FIGURE 1. An overview of on-road EVs in the past decade [21].

FIGURE 2. Governments and customers spending on EVs [22].

system (EMS), and large scale load scheduling and optimization. Finally, Section X concludes the paper.

II. CURRENT TRENDS, ECONOMIC INCENTIVES, BATTERIES TECHNOLOGY AND CHARGING INFRASTRUCTURE

The modern era of EVs started with the mass-level production by General Motors in 1996, and the launch of the Tesla Inc. Model III has opened new horizons for EVs. Some of the recent trends, initiatives, and technological evolutions are presented below:

A. CURRENT TRENDS

After a decade of rapid growth, EVs have surpassed their conventional counterparts in terms of the total cost of ownership. The number of on-road EVs crossed the 10 million mark in 2020. As illustrated in Fig. 1, China led the market with 5.4 million EVs, followed by the European Union (EU) and the United States (US), respectively [21]. Consumers spent approximately $120 billion on EVs in 2020, and governments worldwide have pledged $14 billion in subsidies. Although, incentives for EVs have been reduced from 22% of total expenditures in 2015 to 10% in 2020, as per the statistics shown in Fig. 2 [22]. Almost 3 million new EVs were registered for the first time in a single calendar year, in 2020. Despite the economic downturn during the pandemic, the EU emerged as a global leader with 1.4 million new registrations due to two policy initiatives: 1) 2020 was the target year for the EU's CO_2 emissions rules, which regulated the average CO_2 emissions per kilometer (km) driven by new vehicles. 2) In response to the pandemic's impact, several EU governments increased EV subsidies as a part of their stimulus packages.

B. ECONOMIC INCENTIVES

The economic compensation packages offered by various countries on the purchase of an EV vary from tax incentives to rebates and significantly contribute towards making EVs more accessible and affordable to users. Some of these perks are: 1) In the US, a consumer can get a $7, 500 tax credit
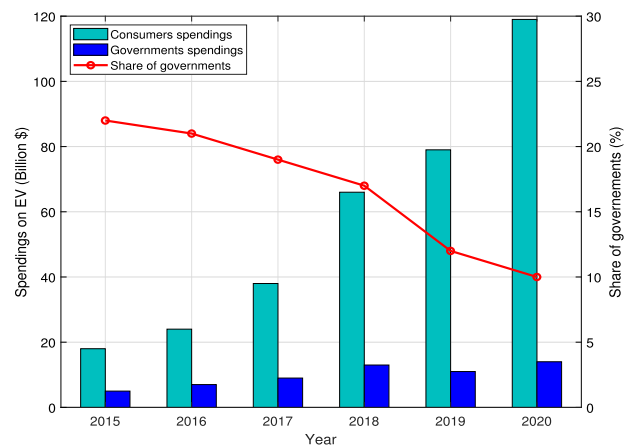
to purchase one of the first 200 k EVs produced by any EV manufacturer. 2) China has boosted its high EV purchase figures with several significant incentives. Such as, a subsidy of ¥25,000 per EV is provided for EVs having a driving range of 400 km or above. Besides that, Chinese EV drivers are exempted from the registration restrictions and driving bans imposed on gasoline vehicles in large cities. 3) In the EU, Norway is one of the frontrunner countries regarding incentives and the total number of on-road EVs. EVs are exempted from the local import tax and the 25% value-added tax. EV drivers can use local bus lanes in congested city areas with reduced ferry crossings and parking charges. Other countries in the EU also offer numerous incentives, such as Germany and Italy providing incentives of € 4,000 per EV. In France, an EV user can receive a purchasing incentive of up to € 8,500. Similarly, EV drivers in the United Kingdom (U.K.) are eligible for a £3,500 rebate on an EV purchase. 4) New Zealand (NZ) is the latest country to offer incentives to EV drivers in the form of cash rebates up to NZ$8,625 [23].

C. BATTERIES TECHNOLOGY

The journey towards e-mobility started with lead-acid batteries; presently, Li-ion batteries dominate the market. Among them, lithium cobalt oxide (LCO) is one of the most mature technologies with the highest volumetric energy density [24]. However, it becomes an expensive choice due to its lower power density, service life, and reliance on precious cobalt elements. On the other hand, lithium iron phosphate (LFP) batteries offer a very long life span and a high power density. However, this technology is less suitable for high-energy applications such as EVs due to its inherent low potential and specific capacitance [25]. The lithium nickel cobalt aluminum oxide (NCA) and lithium nickel manganese cobalt oxide (NMC) variants of Li-ion batteries provide high energy densities and remain the most common option for EV manufacturers. The current trend in NCA and NMC technologies is to reduce the amount of cobalt in favor of nickel in cathodes without affecting the energy density [26]. According
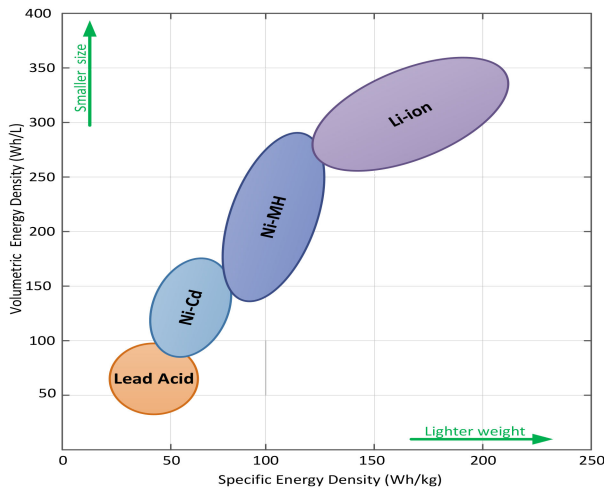
FIGURE 3. An illustration of specific energies and energy densities of various batteries.

FIGURE 4. Slow EVSEs installed in EV-concentrated regions [33].

FIGURE 5. Fast EVSE installed in EV-concentrated regions [34].

to the components' stoichiometric ratio, commercially available NMC battery models include NMC-333, which has all elements in the same proportion; NMC-532; NMC-622; and NMC-712. The relationship between the specific energy and energy density of various battery technologies is illustrated in Fig. 3.

The afore-stated variants of Li-ion technology are based on cathode materials. For anode materials, the options are minimal, and due to the low potential and suitable specific capacitance as compared with Li+, carbon-based anodes such as amorphous carbon and graphite are dominating the market [27]. Presently, the share of graphite anodes is 91%, amorphous carbon is 7%, and lithium titanate oxide (LTO) occupies only 2%. Although LTO supports UF charging and has a longer lifespan, the raw material is costly and also poses a lower energy density [28]. On the other hand, Si is emerging as a potential option for anode material because it is cheaper and has a theoretical capacity tenfold greater than graphite. Although pure Si has a relatively shorter lifespan, research is going on to develop Si-based alloys with an extended lifespan and higher energy densities [29].

With technological advancements, the next generation of Li-ion batteries will have a cell-level energy density of up to 325 Wh/kg, and pack-level energy density may reach 275 Wh/kg [30]. In this regard, solid electrolytes have been extensively studied because their non-toxic and non-flammable characteristics will also lead to substantial improvements in safety. Solid electrolytes minimize voltage losses due to concentration polarization. They have excellent dendritic resistance, which results in higher energy densities [31]. Solid electrolytes for EVs must have rapid charging characteristics. The critical current density is one of the factors that determines the battery's ability to be charged quickly. The desired critical current density of 5 mA per centimeter square (mA/cm^2) is still far away, as state-of-the-art solid electrolytes have a critical current density of 0.1 mA/cm^2 [32].
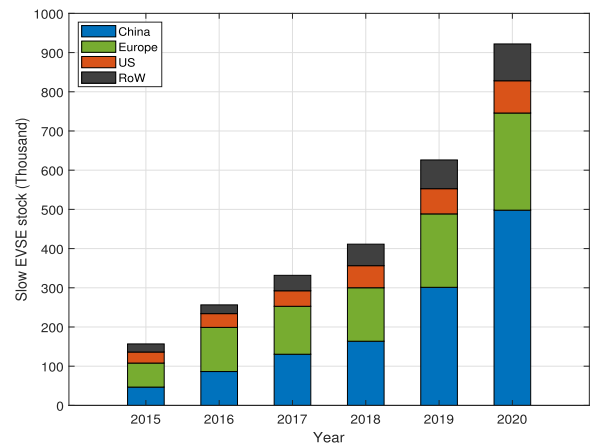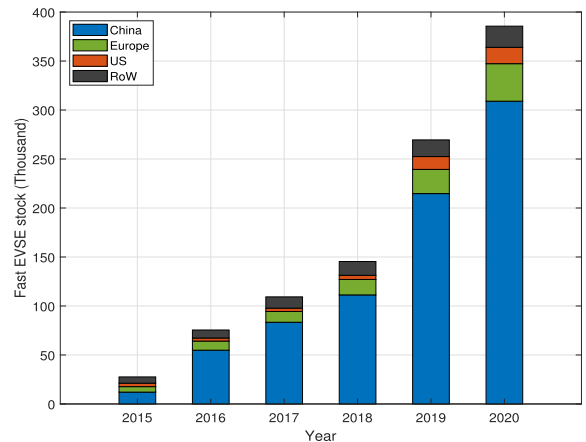
D. CHARGING INFRASTRUCTURE

Although most of the charging takes place at home or the workplace, the availability of public charging facilities will be critical for countries leading in EV adoption since consumers will demand a more convenient and efficient charging infrastructure. Presently, China is the global leader in slow and fast chargers deployments.

By December 2020, the number of slow chargers installed in China was about 0.5 million. Similarly, in the EU and US, slow chargers installation was raised to 0.25 million and 82,000, respectively. Fig. 4 shows the recent statistics of slow EVSEs deployed globally [33].

The rate of fast chargers deployment in China increased by 44% in 2020. The total number of installed chargers was raised to 0.31 million. Similarly, fast chargers are installed more rapidly throughout Europe, and total deployment reached 38,000. The US had 17,000 fast chargers, roughly 60% of which are Tesla superchargers till December, 2020. Fig. 5 illustrates the recent statistics of fast EVSEs deployed globally [34].
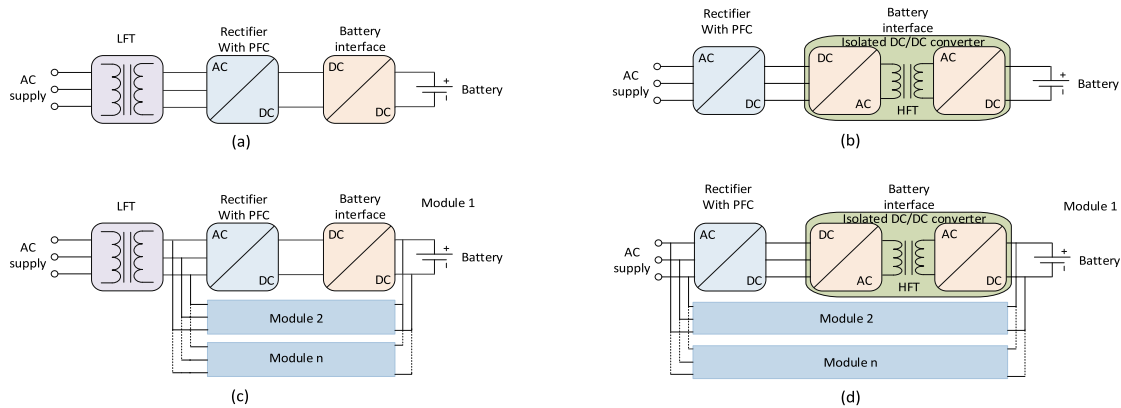
FIGURE 6. Block diagrams of LFT and SST-based DC fast chargers. (a) A single-module charger based on LFT. (b) A single-module charger based on SST. (c) A charger based on LFT with multiple modules connected in parallel. (d) A charger based on SST with multiple modules connected in parallel [39].

However, the majority of EU nations were unable to meet the targets established by the alternative fuel infrastructure directive (AFID) for charging infrastructure [35]. As per the directive, it was recommended that each member country should ensure the availability of at least 1 public charger per 10 EVs by December 2020. Although the average ratio of public EVSE-to-EVs in the EU is 0.09, only the Netherlands and Italy are leading with ratios of 0.22 and 0.13, respectively.

III. EV CHARGERS AND STANDARDS
An EV's charger normally controls and processes electric current to assist energy flow into an EV's battery, and its requirement originated as a result of the AC power availability from the electric grid, whereas EVs require DC power. It mainly consists of an AC/DC converter that converts AC power into the required DC power. A DC/DC converter is also incorporated to optimize energy conversion for fast charging. The EV chargers are categorized into AC (on-board) and DC (off-board) chargers. The AC chargers are also known as slow chargers, while the DC chargers normally have a higher power rating than their AC counterparts and are further divided into fast and UF chargers. Botsford and Szczepanek [36] defined "*fast charging*" as anything that is not slow charging, but such a definition leaves confusion about what exactly is slow charging. The California air resources board (CARB) defines it as "*a charger that enables the vehicle to travel for 100 miles in 10 minutes*" [37].

State-of-the-art DC fast chargers convert the three-phase (3-ϕ) AC supply into the required DC supply via two conversion stages: 1) an AC/DC conversion stage with PFC; 2) a DC/DC conversion stage to regulate the intermediate output DC voltage to the required level for EV charging. As per IEEE standard, 1547 [38], the galvanic isolation between the grid and the EV battery can be provided either by an LFT, as shown in Fig. 6(a), or via an high-frequency transformer (HFT) inside an isolated DC/DC converter, as illustrated in Fig. 6(b). To raise the power rating, multiple identical modules may be connected in parallel to reach the desired power rating, as shown in Fig. 6(c) and (d) [39]. For instance, the Tesla supercharger, which consists of 12 paralleled modules to reach

the desired 135 kW power rating [40]. Some state-of-the-art DC fast chargers are summarized in Table 1.

To ensure compatibility among different EVSEs and EVs, several organizations, such as the society of automotive engineers (SAE) [41], the international electrotechnical commission (IEC) [42], charge de move (CHAdeMO) [43], and Tesla Inc., etc., are working to standardize the EV chargers and connectors. Some of the commonly adopted standards are presented in Table 2.

Moreover, the establishment of international standards and universal connectors, as well as suitable charging infrastructure, is strongly tied to the widespread adoption, growth, and seamless operation of EVs [44]. Protection, safety, batteries, connectors, grid interconnection, and isolation are among the several aspects of and related to EVs that have been addressed by different standards, as presented in Table 3.

IV. UFCS MOTIVATION AND CHALLENGES
Demand for close driving range to gasoline vehicles has evolved EVs, and the majority of EVs nowadays have a driving range of more than 200 miles. Some of the best-selling EVs regarding battery capacity and range per charge has been summarised in the Table 4. The driving range of the EVs available on the market is sufficient in most driving scenarios. However, a UFCS infrastructure capable of replenishing an EV's battery at a rate comparable to gasoline refilling is urgently needed for the widespread adoption of EVs and for meeting the NZE goal. A 7.2 kW level 2 onboard charger takes more than 500 minutes to extend an EV's range by 200 miles, with an estimated consumption of 0.3 kWh/mile. Similarly, a 50 kW DC fast charger and a 135 kW Tesla supercharger can accomplish the same task in 75 and 27 minutes, respectively. Moreover, the recently proposed 350 kW UF charger reduces the refilling time to less than 10 minutes and makes it much more comparable with the refueling time of fossil fuel vehicles, Fig. 7 shows the charging times of AC and DC chargers to refill a 60 kWh battery. From the safety point of view, the cable weight of a 50 kW fast charger is almost 9 kg, and the cable weight of a 350 kW UF charger exceeds the safe weight lifting limits defined by the occupational health

TABLE 1 Specifications of State-of-the-Art DC Fast Chargers [39]

Manufacturer	Model	Power (kW)	Input voltage (V)	output voltage (V)	Output current (A)	Efficiency	Time to add 200 miles
ABB	Terra 53	50	480 AC	200-500 DC 50-500 DC	120	94%	
Tritium	Veefil-RT	50	380-480 AC 600-900 DC	200-500 DC 50-500 DC	125	> 92 %	72
PHIHONG	Integrated Type	120	380 AC ± 15% 480 AC ± 15%	200-750 DC	240	93.5%	30
Tesla	Supercharger	135	380-480 AC	50-410 DC	330	91%	27
EVTEC	Espresso	150	400 AC ± 10%	170-500 DC	300	93%	24
ABB	Terra HP	350		150-920 DC	375	95%	10

TABLE 2 Charging Types and Levels

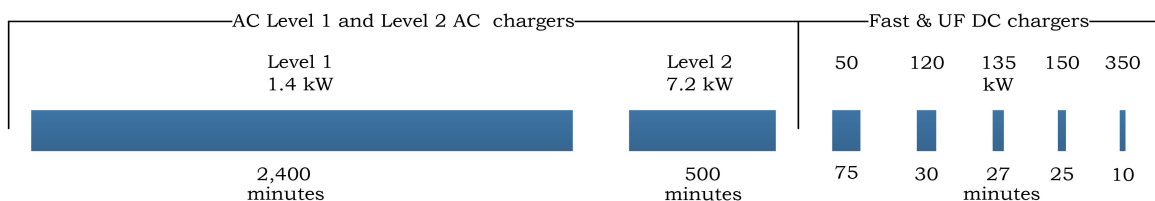| Charging type	Level	Charger location		Time required to recharge a 60 kWh battery (Hours)	Specifications		
		On-board	Off-board		Voltage (V)	Current (A)	Power (kW)
	SAE AC charging Standards						
AC	Level 1	✓	-	7-17	120	12-16	≤1.92
	Level 2	✓	-	0.4-1.2	240	80	1.92 - 19.2
	Level 3	-	✓	0.5-1	480	≥100	≥ 50
	IEC AC charging Standards						
	Level 1	✓	-	2-3	250-450	16	4-7
	Level 2	✓	-	1-2		63	22
	SAE DC charging Standards						
DC	Level 1	-	✓	0.4-1.2	2200-450	80	36
	Level 2	-	✓	0.2-0.4		200	90
	Level 3	-	✓	0.2	200-600	400	240
	CHAdeMO DC charging Standards						
	Fast charging	-	✓	≥0.5	500	125	60
	Tesla supercharger						
	Fast charging	-	✓	≥0.5	≤480	200	≥135

FIGURE 7. Time required by AC and DC chargers to recharge a 60 kWh battery [91].

and safety administration (OSHA) at the voltage level of 400 VDC [45]. Hence, power transfer at higher voltage levels is one of the promising approaches to minimize cable weight and maximize power delivery [46].

On the other hand, designing and deploying a UF charger with such high power and voltage ratings is expensive and complicated, particularly in the case of an MV connection. It must consider the competing industry standards, available technologies, grid impacts, and other technical and policy issues. Installing a single UF charger in a residential area is

almost impossible due to the associated high power, high voltage, safety concerns, and required capital investment. As the cost of installing a UF charger is determined by the location, the condition and upgrade of the electrical service equipment, the foundation, and the conduits from the source to the service transformer and then to the UF charger [47], in this context, the installation of a single UF charger with a 350 kW power rating becomes prohibitively expensive. Generally, it is more realistic to build a UFCS with multiple UF charging slots beside highways, as there is high demand for UF charging,

TABLE 3 International Standards That Address the Charging Methods, Connectors, Safety, and Isolation of EVs

Technical codes	Brief Description
SAE	
J1772	Conductive charging methods
J1773	Inductive charging methods
J2293	Energy transfer systems
J2836/2847/2931	Communication protocols
National Fire Protection Agency (NFPA)	
NEC 625/626	EV charging systems
NFPA 70	EV and electrical installation safety
Institute of Electrical and Electronics Engineers (IEEE)	
IEEE P1547	Grid interconnection
IEEE P2030	Smart grid inter-operatability
IEEE P1809	Electric transportation guide
IEEE P2690	Charging Network management
IEEE 2030.1.1	DC fast charging
International Electrotechnical Commission (IEC)	
IEC TC 21	Battery system management
IEC TC 69	Charging network and safety
IEC 1000.3.6	Power quality issues
Underwriters Laboratories (UL) Inc.	
UL 2594/2251/2201	EVSE
UL 2231	Safety
International Organization for Standarization (ISO)	
ISO 6469-1	Rechargeable battery systems
ISO/CD 6469-3.3	Safety
Japan Electric Vehicle Association (JEVA)	
JEVA C601	Charging connectors
JEVA D701	EV batteries
JEVA G101-109	Fast charging
Deutsches Institut fur Normung (DIN)	
DIN 43538	Batteries systems

and it also makes more economic sense due to reduced capital investment per charging slot.

Aside from the lower capital investment per slot due to multiple charging slots on the same grid-tie equipment, significant research is being conducted to exploit the diversity factor that results from the simultaneous charging of multiple EVs with varying battery capacities and SOCs. For instance, a two-fold optimization algorithm has been proposed in [48]. In the first step, the algorithm aims at profit maximization by providing as many charging facilities as possible. While in the second step focuses on peak power demand reduction by taking the step one objective as a constraint in step two. An on-line optimization algorithm to reduce the station's peak power demand has been presented in [49]. The proposed techniques allow the EV driver to opt between a slow charger with a low charging cost and a fast-charging slot with a high charging cost associated with the charger's power rating.

UFCSs are likely to become major load centers and present challenges to the distribution network. As a function of the batteries capacities and SOCs, charging multiple EVs may cause significant variations in the UFCS instantaneous power demand, and uncoordinated charging scenarios may create peaks in the daily load profile, resulting in detrimental impacts on the distribution system's stability, voltage imbalances, and compromised power quality. Smart charging techniques are presented in [50]–[54] for greater control over EV charging while improving grid stability. However, these techniques are appropriate only for overnight Level 1 and Level 2 home charging scenarios because there are enough time slots to schedule the EVs. In contrast, drivers opting for UF charging need an immediate high-power charge upon plugging their EVs in. Therefore, integration of RESs and ESSs into UFCSs is one of the possible mechanisms to mitigate the high power demand [55]–[57]. Because of the integrated RES and ESS, UFCSs can not only have on-site generation but also provide ancillary grid services like load shifting, voltage and frequency regulation [58]–[60], reactive power compensation [61], [62], and grid firming [63], [64]. Examples include a Tesla supercharger in Mountain View, California, with 400 kWh of battery storage capacity. In [65], authors demonstrate that it is possible to meet over 98% of power demand with an average delay of less than 10 seconds by integrating an ESS and taking the real arrival times and distribution of EV batteries' SOC as well as capacities into account. Section VI discusses the advantages of incorporating RESs and ESSs into the UFCS.

Another approach that has been proposed in the literature is the coordinated charging method. The actual power demand from the grid may be significantly reduced by using the proper coordinated charging strategy to schedule multiple EVs in a single or multiple UFCS. In this regard, state-of-the-art Internet of Things (IoT) based intelligent transportation system (ITS) techniques, such as vehicle-to-vehicle (V2V) and vehicle-to-infrastructure (V2I) communication, can play a vital role in communicating data between EVs and road infrastructure via machine-to-machine (M2M) and message queuing telemetry transport (MQTT) protocols. By equipping EVs and UFCSs with IoT technology capable of sending, receiving, and processing data, it is possible to route EVs towards UFCSs with available capacity or those with the most negligible impact on the power grid manage EVs charging conveniently.

In [66], the authors examine the publish/subscribe (P/S) communication architecture for EVs, roadside units (RSUs), and UFCSs. The RSUs work as communication gateways between the EVs and the UFCSs, assisting the EVs to find and reserve a slot in the least crowded stations. It is more expensive to install and maintain RSUs, and it is impractical to place RSUs at every junction in-vehicle ad-hoc networks. Additionally, the optimum RSUs deployment is very stiff and inflexible. Instead of RSUs, public transportation buses (PTBs) may act as brokers between the message publisher (i.e., UFCS) and the subscriber (i.e., EV), assisting EVs in

TABLE 4 Technical Specifications of Some of the Best-Selling EVs.

Manufacturer	Model	Battery Specifications				Driving range per charge (Miles)	Maximum charging power (kW)
		Chemistry	Capacity (kWh)	Energy density (kWh/L)	Weight (kg)		
Volkswagen	e-golf	NMC-333	35.8	103	349	186	40
Nissan	leaf	NMC-523	62	151	410	186	50
Peugeot	e-208		50	140	356	225	100
Audi	e-torn	NMC-622	95	136	700	274	265
BMW	i3/i3s		42.2	152	278	246	50
Hyundai	Kona electric		67.5	149	258	484	75
Jaguar	i-pace		90	149	603	292	350
Kia	e-soul		64	148	457	280	77
Mercedes	EQC		85	130	652	259	110
Porsche	Taycan		93.4	148	630	280	270
Skoda	Citigo E iv		36.8	148	248	160	40
Chevrolet	Bolt EV	NMC-712	68	158	410	259	50
Renault	ZOE		54.66	168	326	239	50
Tesla	III	NCA	102.4	162	630	315	150

determining the shortest path to their destination [67]. The P/S-based communication architecture comprises three network entities: 1) The UFCS is a stationary charging station that charges EVs in parallel by utilizing multiple charging slots. 2) PTBs are mobile entities that act as intermediaries, transmitting UFCS data to and from EVs. 3) EVs act as subscribers, receiving published information or demanding its release. All legitimate PTBs engaged in information dissemination receive frequent broadcasts from each UFCS about its current status. All UFCS released information will be gathered by each PTB and cached for later use. If the PTB receives new information, it will overwrite the old cached data. Distributed charging management is well-suited to the P/S communication architecture because EVs may use the condition information from opportunistically encountered EVs to make charge management choices for their own UFCSs. Depending on the charging needs in certain locations, the PTB cloud may be dynamically created. From a practical standpoint, the European telecommunications standards institute (ETSI) TS 101 556-1 [68] and the ETSI TS 101 556-3 [69] assist implementation from a practical standpoint.

V. UFCS ARCHITECTURES

A state-of-the-art UFCS requires a $3-\phi$ MV grid connection, and the incoming voltage is step-down either by an MV/LV LFT or an SST to the operating voltage of a UF charger. The bus bar of a UFCS to accommodate multiple UF chargers, local RESs, and ESSs may be designed either as a standard AC or DC bus. Each approach has several advantages and challenges, as discussed below.

A. AC BUS DESIGN

In AC bus design, a step-down-transformer connects the MV grid to the standard AC bus of a UFCS. Each UF charger is connected to the AC bus via separate AC/DC and DC/DC converters to ensure a regulated DC voltage for an EV's battery charger. Furthermore, the on-site RES and ESS are interconnected to the AC bus through DC/DC and DC/AC converters, as illustrated in Fig. 8(a) [70]. However, the use of dedicated AC/DC and DC/DC converters for each load (i.e., UF charger and ESS) and source (i.e., RES and ESS) substantially increased the conversion stages, resulting in increased cost, complexity, and reduced efficiency. The AC bus design provides several benefits, such as mature AC/DC and DC/AC conversion technology, well-established standards and procedures for AC distribution systems, standardized AC switchgear, and protective relays [71]–[73]. Furthermore, separate standards for common AC bus charging stations have already been developed and implemented in state-of-the-art UFCSs such as the Tesla supercharger station in Mountain View, California, and the ABB DC fast-charging station in Europa, Victoria, Australia [74].

B. DC BUS DESIGN

A common DC bus design, as illustrated in Fig. 8(b), consists of a central DC/DC converter after LFT and provides a more efficient approach for interconnecting multiple UF chargers, RES, and ESS to a common DC bus via DC/DC converters [75]. In contrast to AC bus design, this approach eliminates the individual AC/DC converters required for each load and source, with improved system efficiency and reduced cost. The DC bus should be designed at a voltage level of less than 1 kV to reasonably insulator cost safety concerns and to support the state-of-the-art batteries voltage ranges. At this voltage level, a DC bus UFCS should comply with the same standards as a UFCS on an AC bus [71]–[73]. A key benefit of DC bus design is a single point of coupling with the MV grid that simplifies the grid-connected and islanded operation
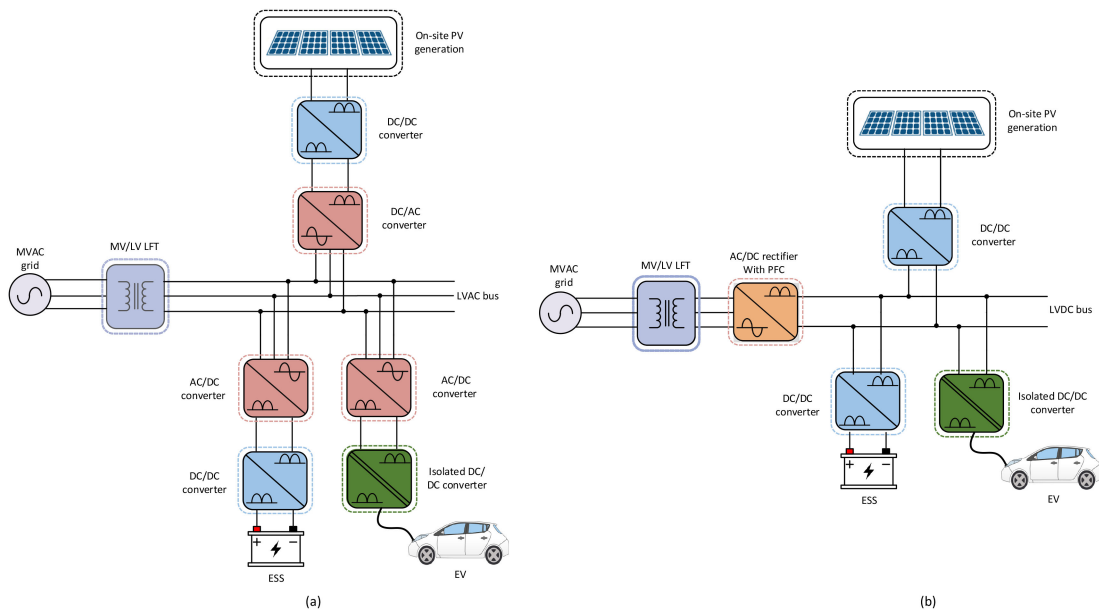
FIGURE 8. An UFCS's LFT-based architectures. (a) A typical AC bus design. (b) A typical DC bus design.

modes. Other advantages include the lack of reactive power, being easy to control [76], and the use of partial power converters [77]–[80]. The fact that the partial power converters process just a portion of the power required for an EV reduces the size and cost of the converters while increasing conversion efficiency [81].

1) MEDIUM/HFT BASED DC BUS DESIGN
Due to the lack of a DC transformer, the presence of a bulky MV/LV LFT is required, as illustrated in Fig. 8, resulting in increased capital investments, size, and complicated design to interface the incoming power and provide the required isolation between the AC and DC sections. A Medium/HFT (M/HFT) inside an isolated DC/DC after the front-end AC/DC converter can replace the bulky LFT to interface with the MV grid while providing the required isolation as per IEEE 1547. Numerous M/HFT-based configurations of the DC bus are presented in Fig. 9. A unidirectional architecture is illustrated in Fig. 9(a), where the input AC voltage is rectified by a front-end, followed by a non-isolated DC/DC converter with power factor correction (PFC) features, and finally, an isolated DC/DC stage. Fig. 9(b) shows an alternate architecture that reduces not only the number of conversion stages but also improves the overall conversion efficiency with combined isolation and PFC stages. A bidirectional architecture, as shown in Fig. 9(c), consists of an active front-end (AFE) to provide PFC with AC/DC conversion by controlling the active switches with pulse width modulation (PWM) and a DC/DC isolated converter. Besides bidirectional features, its key benefit over the prior architectures is that the second stage requires a small-sized isolated DC/DC converter with improved efficiency and reduced cost [82], [83].

Regardless of its benefits, a DC bus design introduces new challenges like DC protection and metering. Although DC

fault detection and isolation devices such as fuses, circuit breakers, solid-state (SS) circuit breakers [84], and relays [85] are available, no well-established standards for coordination protection have been developed yet. Due to the low inertia of DC systems, they are vulnerable to disturbance and may become unstable in the absence of rapid fault clearing mechanisms. Consequently, the speed with which faults are detected and isolated is crucial for system recovery. Studies of the DC distribution systems, such as LVDC microgrids, guide the coordinated protection of DC UFCSs. [86] presents a protection approach for an LVDC microgrid that takes into account the synchronization of several protective devices. Reference [87] proposes a protection strategy for DC systems using a loop-type bus. The proposed techniques can detect and isolate faults while maintaining a continuous power supply.

VI. INTEGRATION OF ESS AND RES
It is not always feasible to have a strong grid connection alongside the highways and rural areas. According to research by the California public utilities commission [88], as the UFCSs network expands, the distribution network will require much more upgrades than the generation and transmission sectors. For example, a typical highway UFCS with two 350 kW and four 150 kW chargers will introduce additional power demand 1.3 megawatts (MW). They will need an upgraded distribution transformer and associated infrastructure. In Norway, grid upgrading is projected to cost $1.6 billion to manage the irregular charging behaviors of the massive number of EVs anticipated to be on Norwegian roads by 2040 [89]. However, by sharing upstream equipment across several EVSEs, the site's construction and network up-gradation cost can be distributed over the charging slots. The capital investment per slot may be substantially minimized.
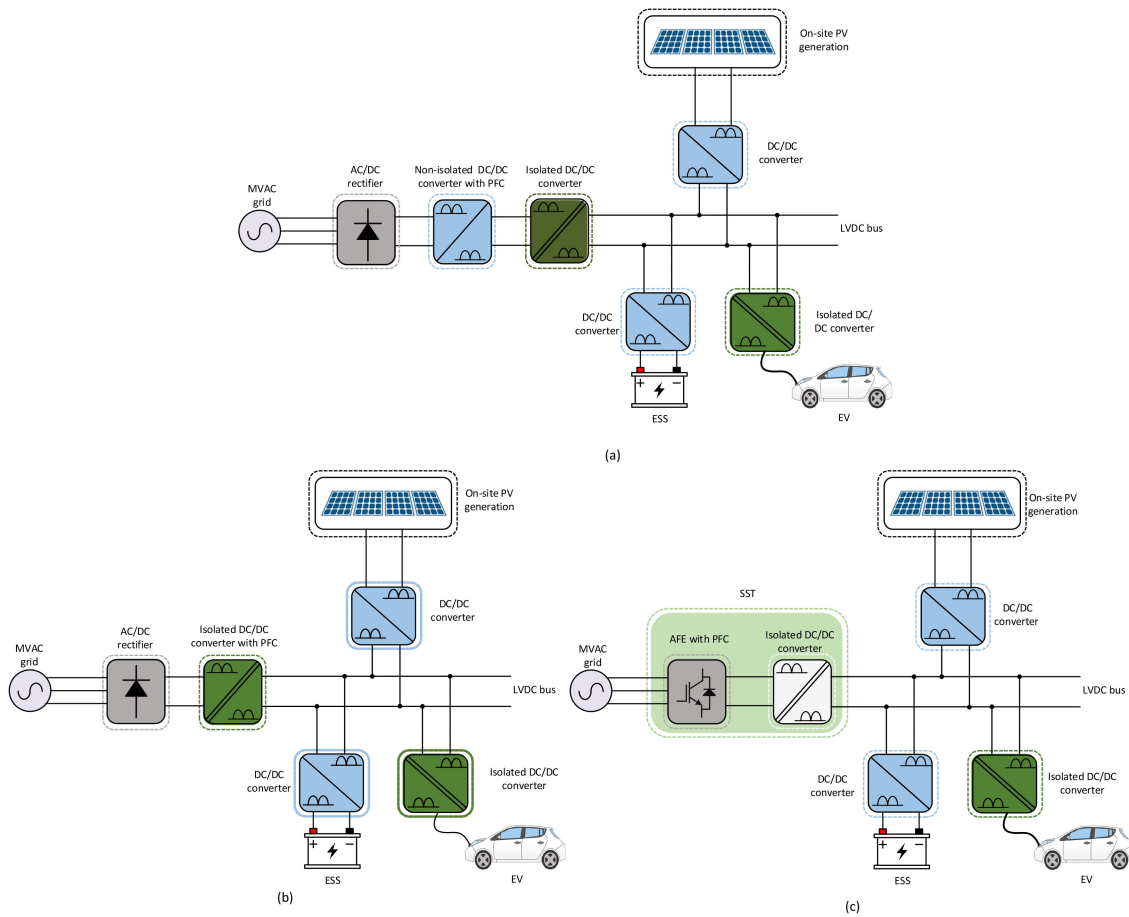
FIGURE 9. An UFCS's M/HFT-based common DC bus architecture. (a) Unidirectional design with separate PFC and isolation stages. (b) Unidirectional design with combined PFC and isolation stages. (c) Bidirectional design with AFE and isolation stages.

Apart from the substantial capital investment, the high power demand of UFCSs results in high operational costs, as utility companies charge non-residential customers based on peak demand measured in kW, along with fixed monthly connection charges and actual energy consumption charges measured in kWh, making them unattractive to investors [90]. The peak demand charge is defined in [91] as *"a demand charge is a fee based on the highest rate, measured in kW, at which electricity is drawn during any 15-to-30 minute interval in the monthly billing period."* It is considered a kind of compensation for the deterioration of power plants, transmission and distribution lines, transformers, and other utility equipment located between a consumer's premises and the service provider. In the US, peak demand charges vary from $2 per kW to $90 per kW [92]. For instance, a UFCS with three 150 kW charging slots, a consumption price of $0.1/kW, a fixed monthly connection fee of $140, and a peak demand charge of $45 per kW. Besides, the fixed monthly charges of $140 and actual energy consumption charges of $150, $300, and $450 in the case of no, two, and three simultaneous charges. The corresponding monthly demand charges for the three possible scenarios will be $6,750, $13,500, and $20,250, respectively. A breakdown of the operational expenses is depicted in Fig. 10.

To keep the monthly peak demand fees as low as possible while retaining the ability to provide three concurrent charges. An ESS with a high power density and efficiency and corresponding power electronics converters will be required. Based on a 90% roundup efficiency and only 10% charging, self-discharge, and discharging losses, the minimum ESS capacity to perform three simultaneous charges at 150 kW for 20 minutes is approximately 170 kWh. The utility may recharge the ESS using a 17 kW level 2 AC charger, but it will take 10 hours to recharge the ESS fully. A more realistic approach would be to use a 50 kW DC fast charger to obtain 100% SOC in 3.4 hours. The corresponding power demands of a UFCS in the presence and absence of an integrated ESS are shown in Fig. 11. In the presence of an ESS, the UFCS peak demand charges will be $765 and $2250, with a 17 kW and a 50 kW charger, respectively, in addition to the fixed monthly connection fee of $140 and consumption fee of $510, as illustrated in Fig. 12.

The integration of an ESS and the associated power electronics interfacing will require an additional capital investment. According to the cost estimation of $390/kWh as presented in [93], the required 170 kWh ESS will cost $66,300. Directly related to the EV charging scenarios and power rating of the ESS charger, savings in monthly
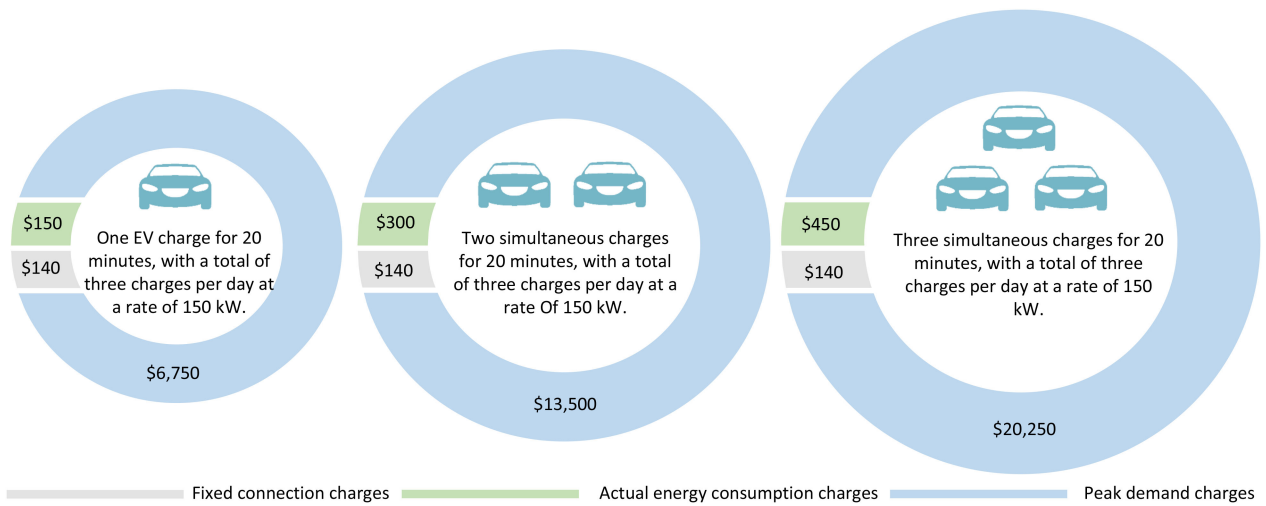
$150
$140
One EV charge for 20 minutes, with a total of three charges per day at a rate of 150 kW.
$6,750

$300
$140
Two simultaneous charges for 20 minutes, with a total of three charges per day at a rate Of 150 kW.
$13,500

$450
$140
Three simultaneous charges for 20 minutes, with a total of three charges per day at a rate of 150 kW.
$20,250

Fixed connection charges — Actual energy consumption charges — Peak demand charges

FIGURE 10. A breakdown of an UFCS's monthly operational costs in the absence of an ESS.
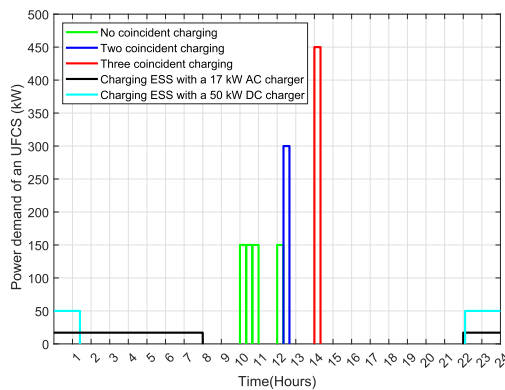

FIGURE 11. Power requirements of an UFCS with three 150 *kW* DC fast chargers, with and without an integrated ESS.
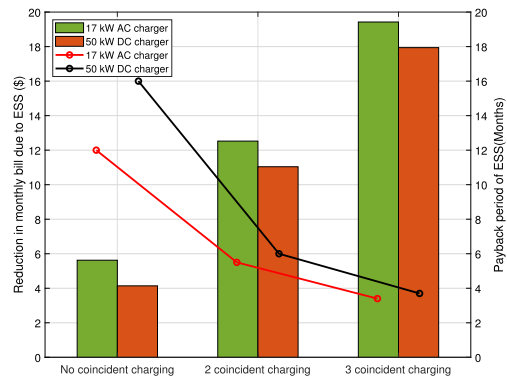

FIGURE 13. Total savings in monthly operational costs and payback period of an integrated ESS.

$510
$510
$140
$140
Charging the integrated 170 kWh ESS either with a 17 kW AC Level 2 or 50 kW DC Fast charger.
$765
$2250

Fixed connection charges — Actual consumption charges of a 17 kW charger — Peak demand charges of a 17 kW charger — Actual consumption charges of a 50 kW charger — Peak demand charges of a 50 kW charger
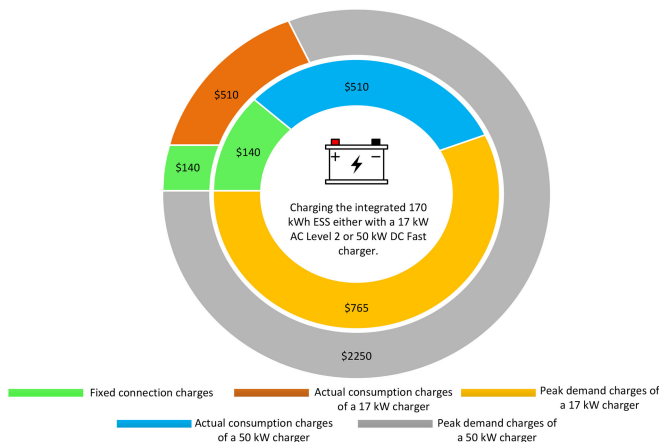
FIGURE 12. A breakdown of an UFCS's monthly operational costs in the presence of an integrated ESS.

operational expenses of the UFCS vary from $1435 to $2900 with a corresponding payback period of 3.4 to 16 months. The reductions in operational expenditures in the cases of a 17 kW AC level 2 charger and a 50 kW DC fast charger with no, two,

or three coincident charges, as well as the associated payback periods, are shown in Fig. 13.

Undoubtedly, e-mobility is a promising technology that can significantly improve the sustainability of the transportation sector while reducing GHG emissions. This objective is only possible if the required electricity comes from RESs. However, it becomes more challenging as RESs are subjected to intermittent nature, and the unpredictable arrival of EVs makes it more complicated. The integrated ESS with RESs can serve as an energy buffer to store the generated energy by RESs for later use. The reference [94] investigates how an ESS is critical in a power system that heavily relies on RESs. By using an ESS [95]–[97], a large-scale photovoltaic (PV) plant's stored energy may be used to improve voltage and frequency stability, as well as provide peak shaving. Some of the ongoing projects are summarized as below:

In Hokkaido, Japan, one of the world's largest battery storage systems, totaling 60 MWh, has been built to integrate solar energy into the grid [98]. Similar initiatives are also being pursued in other countries to increase the efficiency of wind energy integration. For example, in west Texas, a 24 MWh

battery ESS was incorporated into a 156.6 MW wind farm to store energy during off-peak hours [99]. Another comparable but larger (i.e., 32 MWh) Li-ion battery ESS was built in southern California to offer voltage support and frequency control near a 450 MW wind farm [100]. Numerous Power to Gas (P2G) initiatives has been launched to generate hydrogen from surplus renewable energy. For example, E.ON, a German utility, has built a 2 MW P2G plant in Falkenhagen, Germany, in collaboration with Swissgas and Hydrogenics [101]. Reference [102] presented a detailed list of other P2G initiatives in Australia, Canada, China, Germany, Japan, the Netherlands, and the US.

As previously stated, an integrated ESS not only reduces the operational costs of a UFCS but also eliminates the need for distribution network upgrades, allowing UFCSs to be installed in rural areas and alongside highways. Even without considering its application in a UFCS, the real-world examples of ESS presented above are beneficial for providing grid support services. The introduction of an ESS into a UFCS, on the other hand, makes UFCSs appealing to investors by reducing operational costs and providing ancillary grid services. An ESS functions as a virtual power plant and will become an integral part of UFCSs. For example, EVgo, the largest UFCSs network in the US, has integrated ESSs into its 11 UFCSs [103]; Volkswagen uses Tesla ESS in its UFCSs; and Tesla has also introduced the supercharger V3 stations with integrated ESS and on-site PV generation [104].

VII. FUTURE TRENDS, SST AND SST-BASED UFCS

The charging process of an EV with DC fast chargers is much faster than with AC chargers, but it is still slower than a gasoline vehicle's refilling process. As discussed in Section IV, delivering power at high voltage rates, such as 800 VDC, can further reduce the charging time without violating the OSHA, SAE, IEEE, and IEC standards that define the cable weight and current limits for different charging levels and connectors, as illustrated in Table. 2. Besides UFCSs, switching to high voltage will result in reduced volume and weight of an EV's power-train, as explained in Section I. In this regard, manufacturers like Aston Martin and Porsche have announced the production of EVs with an 800 V batteries and associated power-trains [105], [106].

As the number of EVs increases exponentially, so do the corresponding charging requirements and deployments of EVSEs, as shown in Figs. 4 and 5. However, the provision of charging facilities from the LV network will adversely impact the distribution network. To accommodate state-of-the-art EVs, extensive research is required to design UFCSs with dedicated MV connections and an internal DC bus of 800 VDC. A common DC bus architecture for MV-connected UFCSs is presented in Fig. 8(b). However, studies [107]–[110] have proposed the use of SST for UFCS applications to reduce the footprint and improve controllability as well as efficiency in the case of light load. Besides that, SST poses numerous advantages over conventional LFT, some of the SST functionalities include: 1) Protects load from Power

System disturbance, 2) Protects Power System from load disturbance, 3) DC port for ESS & RES integration, 4) Redundant & fault-tolerant structure, 6) Definable output frequency, 6) M/HFT isolation, and 7) Supervisory control/status monitoring interface. Moreover, an illustration of SST and LFT for AC/AC and AC/DC applications has been presented in Fig. 16. In this context, Fig. 9 depicts unidirectional and bidirectional M/HFT-based architectures for MV-connected UFCSs. Moreover, the use of ESS as presented in Section VI will be valuable to reduce a UFCS power demand and demand charges and provide ancillary grid services and ensure UFCS's smooth operation in grid-connected and islanded modes. M. Vasiladiotis et al. [111] examines modular ESS solutions for SST-based architectures, and [112] summarizes various power converters for grid integration of battery ESS.

A. SST

A SST performs the MV/LV transformation like an LFT through AC/DC, DC/DC, and DC/AC conversion stages while providing the required isolation but with improved convertibility and controllability. SSTs are classified as single-stage, two-stage, or three-stage topologies based on the number of conversion stages, as shown in Fig. 14. In contrast to single-stage and double-stage SSTs, the three-stage topology explicitly creates a DC bus to interconnect EVs, ESSs, and RESs. It is one of the most suitable topologies for UFCS applications. It is designed with two DC links, enabling it to provide various functionalities other than single-stage and double-stage topologies. Table 5 contains a functional comparison of all three topologies. In three-stage SST, an AFE interfaces the MV-grid and converts the incoming MVAC into MVDC, followed by an isolated DC/DC stage that transforms the MVDC into the desired LVDC and provides galvanic isolation via an HFT with a much-reduced footprint than an LFT. If auxiliary services are required at the UFCS from SST, an LVDC to LVAC converter can be used at the third stage. Besides numerous indigenous benefits, modularity and the distributed control requirements, on the other hand, increase the control complexity and necessitate whole system synchronization. In this case, hierarchical control with distinct objectives for each stage is the suitable control structure for SSTs, as illustrated in Fig. 15 [113].

Some of the notable publications that addressed different aspects of SST include: [114] provided insights on the design, optimization, applications, and implications for a 15 kV SiC IGBTs-based SST. Liserre, et al. [115], the authors discuss the structural modularity, control strategies, possible functionalities, and challenges to SST. Similarly, Huang, et al. [116] focused on the MV-SST applications and functionalities. In [117], F. Briz, et al. presented a modular multilevel converter (MMC) and cascaded HB (CHB) based MV-SST as one of the possible options for modularity of a three-stage SST. R. Zhu and M. Lissere [118], provided insights on concepts, motivation, as well as functionalities in RESs and EVs penetrated power systems. While focusing on three-stage topology, the SST safety requirements, overload protection,
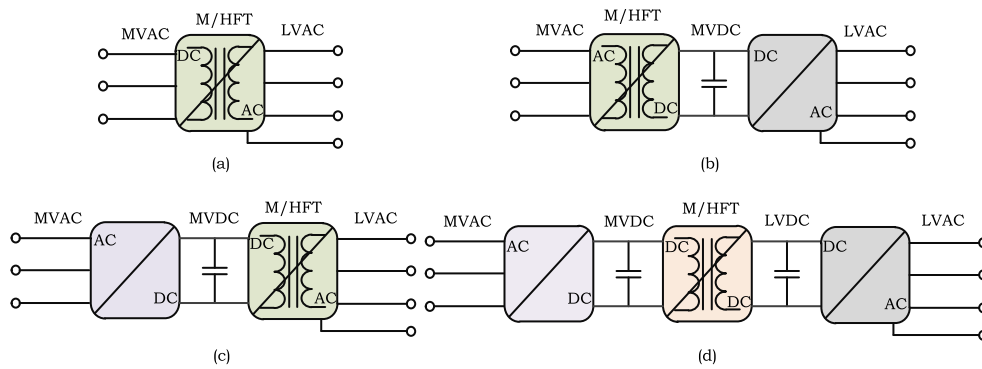
FIGURE 14. SST topologies. (a) Single-stage topology. b) Two-stages topology with LVDC DC-link. (c) Two-stages topology with MVDC DC-link. (d) Three-stages topology with LVDC and MVDC DC-links.

TABLE 5 Functionalities Comparison of SST Topologies.

Functionality	Single Stage	Two Stage	Three Stage
Bidirectional power flow	✓	✓	✓
input current limitation	✗	✓	✓
output current limitation	✗	✓	✓
Reactive power support to the grid	✗	✓	✓
Independent PF	✗	✓	✓
Independent frequency	✗	✓	✓
LVDC undervoltage protection	-	✓	✓
VDC overvoltage protection	-	✓	✓
HVDC undervoltage protection	-	-	✓
HVDC overvoltage protection	-	-	✓
HVDC link regulation	-	-	Good
Output voltage regulation			
Input voltage sag ride through	Poor	Good	Very Good
LVDC link regulation	-		
Input current regulation	✗		
Modularity	Simple	Hard	Simple

connection rules, voltage, and frequency requirements have also been discussed. Similarly, a frequency-based overload control scheme is presented in [119]. A universal power flow control methodology to ensure stable and reliable operation of SST in both radial and meshed configurations without switching the control schemes in the event of faults is presented in [120]. The proposed scheme is validated on the Cigré LVAC benchmark design in Matlab. To avoid the de-rating of SST in overload conditions, a coordinated frequency and voltage control scheme is presented in [121], and the proposed scheme is executed by interacting with local generation sources and loads to provide the necessary support services. Due to the penetration of non-dispatchable generation, an SST-based active power control/support scheme is presented in [122]. The proposed scheme aims to inject reactive power into the grid, reduce the active power demand of voltage-dependent loads in an SST-fed network, and control the SST output voltage to stabilize the voltage before the operation of MV grid tap chargers.

B. SST-BASED UFCS
As an emerging technology, SST can influence various areas, such as the smart grid, UFCSs, RES-penetrated power systems, etc. SST poses some of the common benefits over LFT that include voltage and frequency support services quickly and efficiently as compared to tap-changing of LFT, power quality improvement, fault current limitation and fault isolation, power flow control, and better THD performance [123]. One of the most prominent features that make SST lucrative for portable applications is its reduced weight and size. According to [124], [125], a 3-ϕ SST occupies 80% less space than a conventional LFT. A comparison of SST and LFT for AC/AC and AC/DC applications with respect to Volume, weight, cost and associated losses is illustrated in Fig. 16 [126]. State-of-the-art SST-based UF DC chargers proposed in the literature are summarized below.

A. Maitra *et al.* [127] proposed an MV UF charger topology with symmetrical submodules (SMs) connected in series on the AC side and parallel on the DC side. At the AC/DC conversion and PFC stages, the NPC converter has been used with the internal voltage of each SM set at 1.25 kV, followed by a DC/DC regulation stage, in which PSFB converters with input series and output parallel connections have been utilized. However, a vast number of off-the-shelf Si IGBTs have been used, which results in increased cost and reduced efficiency.
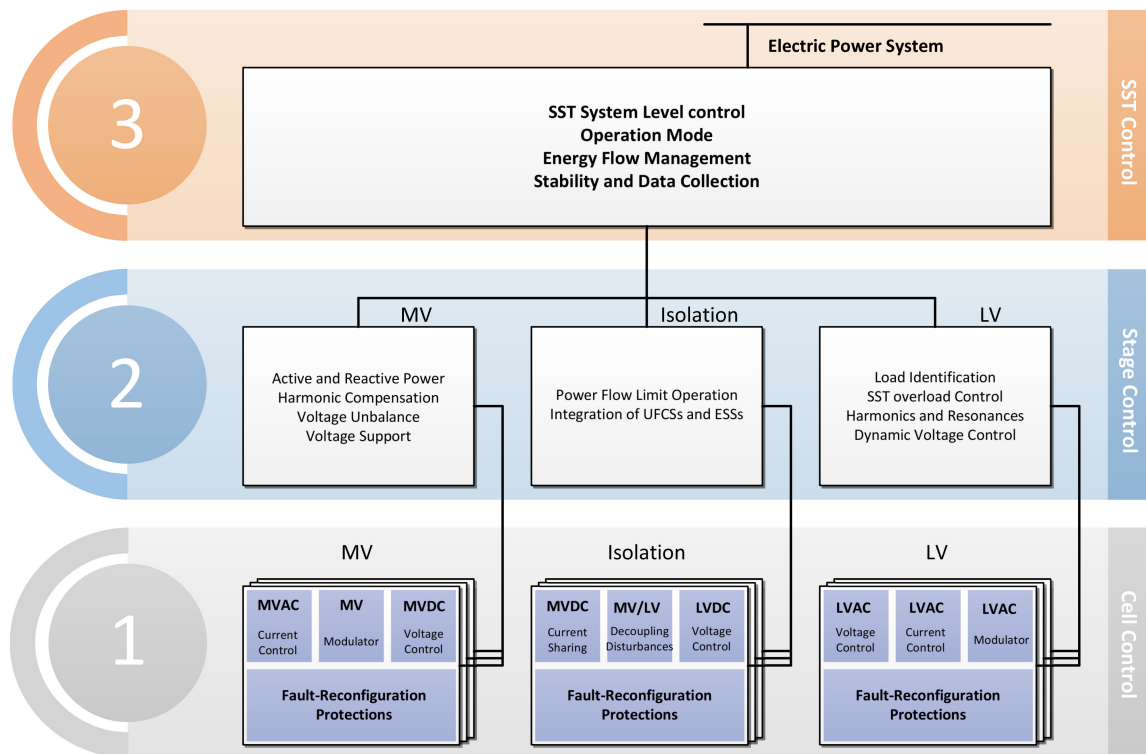
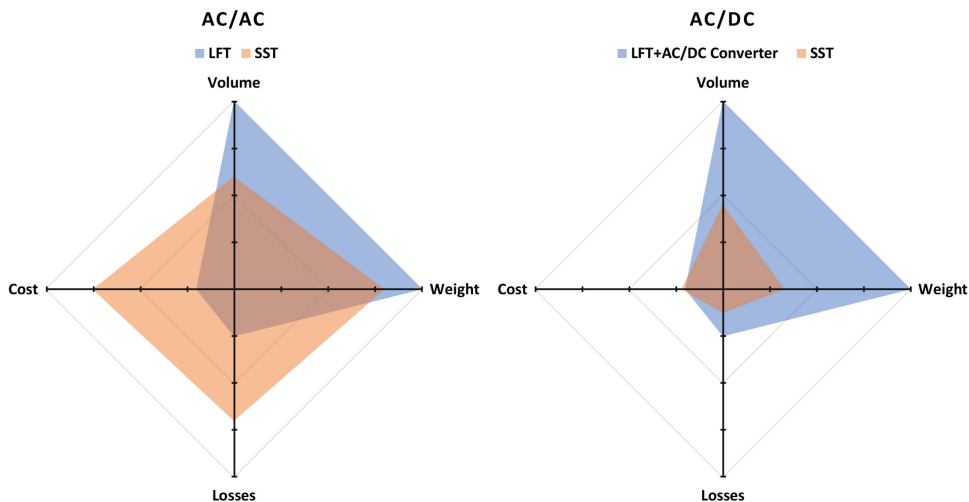**FIGURE 15.** The hierarchical control structure of an SST [113].

FIGURE 16. A comparison of SST and LFT for AC/AC and AC/DC applications with a power rating of 1 MVA, 10 kV AC input and 400 VDC output [126].

A 6-ϕ interleaved boost converter-based UF charger is presented in [128]. The proposed charger was connected to an 8 kV MV line, and eight identical SMs were serially connected to share the input voltage equally. The rectification stage of each SM has an uncontrolled diode rectifier followed by two paralleled unidirectional 3 L boost converters as a PFC stage. The DC/DC regulation stage consists of two HB LLC converters with series and parallel connections at the input and output sides, respectively. The LLC converters are operated in an open-loop with a duty cycle of 100% to achieve the highest possible efficiency. However, this control strategy resulted in a narrow output voltage range, which may not be enough to meet the EV charging requirements. In the case of direct connection with an EV, an intermediate DC/DC converter is mandatory to accommodate the battery voltage range. Furthermore, at a rated load of 25 kW, 97.5% efficiency is achieved.

S. Srdic *et al.* [129] shows a 50 kW UF charger operating at MV. To evenly share the high voltage at the input side,

three identical SMs are connected in series. Despite using a dedicated diode bridge for each SM, a common bridge rectifier is used at the rectification stage. This arrangement reduced the forward voltage drop in the diodes and improved the efficiency. However, it significantly increased the $\frac{dv}{dt}$ ratio at the front end. After rectification, the PFC is performed by a 3 L boost converter. At the DC/DC regulation stage, HB NPC topology with an HFT is used. As stated in [129], one of the main advantages of using NPC is that it further reduces the HFT size. The proposed topology achieved an efficiency of 97.5% at the rated load of 50 kW.

An SST-based implementation is presented in [130]. The proposed topology consists of a FB AC/DC front-end and a DHB DC/DC at the regulation stage. An ESS has been integrated into the UFCS via a non-isolated boost type converter between the rectification and regulation stages. As compared with the topologies mentioned earlier, bidirectional power flow has been achieved in this strategy. However, the use of more active switches results in the under-utilization of the switches and lower efficiency. In contrast to unidirectional power flow, the bidirectional capability makes the control circuitry more complex. A down-scale prototype of the topology with a 140 V AC input has been built and verified in the lab. D. Sha *et al.* [131] proposes a similar design with a FB as AFE and a DAB at the DC/DC conversion stage. Similar to the design in [130], this topology has also been verified at a down-scale level in the lab.

A 400 kW UF charger design project funded by Delta Electronics is presented in [132]. The project aims to design a UF charger using SST and integrate it with a 4.8 or 13.2 kV line. Considering the line-to-neutral voltage, each SM is created at a 15 kW rating with an input voltage of 1 kV. For interconnection with a 4.8 kV grid, three identical SMs are connected in series, and for 13.2 kV, the number of cascaded SMs is raised to 9. Moreover, the AC/DC conversion and PFC are provided by an NPC as an AFE, and an LLC converter performs the DC/DC regulation. A distinguishing feature of the LLC converter used is that it consists of a 3 L converter on the primary side and an active FB on the secondary side. The primary side arrangements reduced the stress on the resonant tank, and the secondary side decreased losses due to synchronous rectification. Higher efficiency is achieved by using SiC MOSFET, but it also significantly raises the cost. A unidirectional model has been developed in the lab to avoid complexity in control. The reported efficiency of an individual 15 kW SM with 1 kV AC input is 97.3%.

VIII. POWER ELECTRONICS CONVERTERS
Power electronics converters are essential components of an EVSE to transform the input AC voltage into an appropriate output DC voltage. There are a variety of AC/DC and DC/DC converters. The power converter topologies that have been extensively researched for EV charging applications, as well as the most suitable topologies for MV-connected UFCSs, are presented below:

A. FRONT-END AC/DC CONVERTERS
Grid-facing AC/DC converters are used to connect an electrical grid to a UFCS's regulated DC bus. A critical performance criterion for front-end AC/DC converters is to guarantee high power quality on both AC and DC sides, which can be achieved with input-current shaping and output-voltage regulation [133]-[134].

To provide charging facilities with a unidirectional G2V power flow feature, the Vienna type-T three-level (3 L) front-end rectifier, as illustrated in Fig. 17(a), is a predominant unidirectional AC/DC converter and has been commercially adopted by many manufacturers due to the reduced number of active switches. It consists of a 3-ϕ diode rectifier to interface with the incoming AC supply and a specific arrangement of active switches that connect each phase to a common midpoint of the DC-link. Its merits include the 3 L characteristics due to the split DC bus and reduced voltage stress on active devices as each switch has to block only one-half of the main line-to-line voltage. On the other hand, it poses the common demerits of 3 L converters, requiring a DC-link capacitor for voltage balancing and having a limited range of attainable reactive power due to a constrained modulation vector and output voltage. The reactive power control range lies between $-30 < \phi < 30$, when the output voltage is greater than twice of the incoming line-to-line peak voltage, whereas the range of attainable reactive power is reduced to $\phi = 0$, when the output and input line-to-line peak voltages are the same. A 25 kW EV charger consisting of a Vienna rectifier at the front-end and four 3 L DC/DC converters at the back-end has been proposed in [135]. Similarly, a 20 kW SiC-based Vienna rectifier with an operating frequency of 140 kHz and 98.6% efficiency due to reduced passive components is presented in [136]. Anderson *et al.* [137], propose an EV charger consisting of a Vienna rectifier at the front-end and incorporating two isolated DC/DC converters at the back-end to equally share the DC bus voltage. By injecting the 6th harmonic into the DC bus via a DC/DC converter and operating only one phase of the Vienna at a time, efficiency is increased.

A buck AC/DC topology, as illustrated in Fig. 17(b), can be utilized if a lower output voltage is required than the incoming line-to-line voltage. This topology poses some prominent features, in contrast, to boost converters, such as in-built short-circuit protection, inrush current limitation, and open-loop control of input current. Although it is a unidirectional topology with a fixed polarity, reverse power flow is possible by changing the polarity. Moreover, the phase shift (PS) of incoming current and voltage directly relates to the output voltage. To maintain a significant PS between the input voltage and current, the converters must be operated in a narrow output voltage range and vice versa. As compared to the boost topology, buck converters have significant conduction losses due to series connections [138]. However, switching losses may be minimized with a design presented in [139], with a reported efficiency of 98.8%.
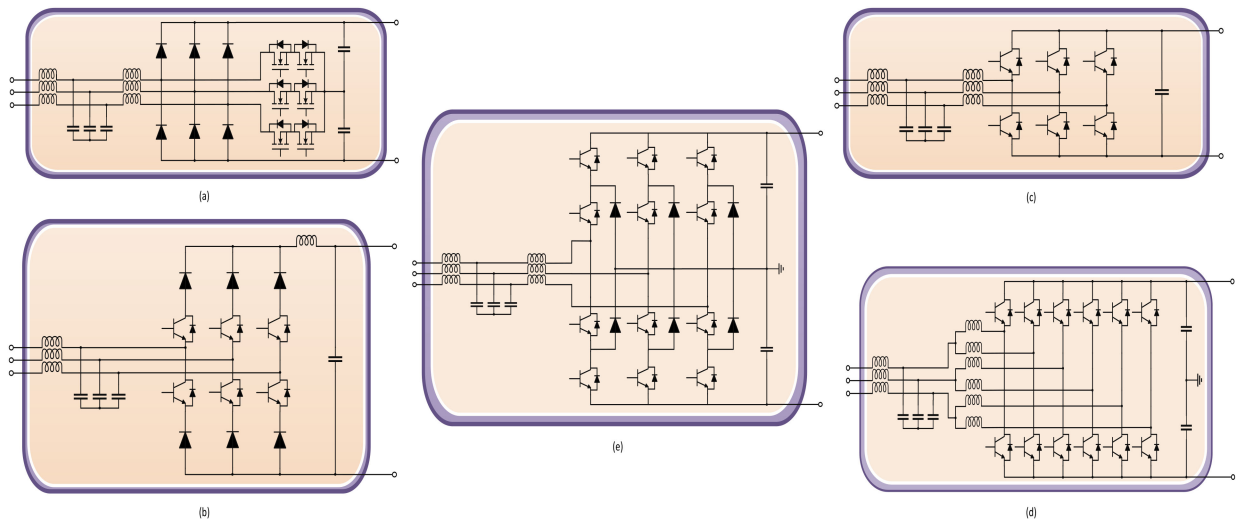
FIGURE 17. Grid-facing AC/DC converters. (a) Vienna Type-T converter. (b) A Buck-type converter. (c) A 3-ϕ PWM converter. (d) An interleaved 3-ϕ PWM converter. (e) A NPC converter.

In the case of bidirectional power flow requirements with G2V and V2G features, the widely used grid-facing AC/DC boost-type converter is the 3-ϕ active PWM converter, as illustrated in Fig. 17(c). It has an output voltage higher than the input line-to-line peak voltage. The six-switch PWM converter generates low-harmonic input currents that provide bidirectional power flow and PFC. Due to the simple structure, well-established control schemes, and the availability of low-cost insulated gate bipolar transistor (IGBT) devices with sufficient current and voltage ratings, it is widely adopted in the state-of-the-art DC fast chargers [140]. An interleaved version, as shown in Fig. 17(d), can be used to increase the current and voltage rating while decreasing the voltage stresses on each switch.

Another boost-type implementation is the neutral point clamp (NPC) converter, as shown in Fig. 17(e). It is one of the most prominent 3 L topologies that has been extensively implemented for numerous industrial applications other than EV chargers. In addition to having a lower $\frac{dv}{dt}$ than traditional two-level (2 L) converters, the harmonic performance is significantly improved. It enables low power rating devices to cascade to achieve the appropriate voltage and power rating. The use of SiC semiconductors eliminates the need for a cascaded structure. It makes MV application possible with improved power density, efficiency, fewer active devices, and simple control. In addition to low total harmonic distortion (THD), partial power converters can process only the necessary power at the DC/DC stage. Furthermore, its inherent bipolar DC property is investigated in [141]–[143] for bipolar DC charging stations.

1) MV FRONT-END AC/DC CONVERTERS

For MV applications, the three most popular front-end topologies are NPC, cascaded HB (CHB), and modular multilevel converter (MMC). Table 6 summarizes their merits, demerits,

applications, active and passive component requirements, and possible structural scalability.

As mentioned earlier, the 3 L NPC converter is one of the most commonly used AC/DC topologies for active power filters, Static Synchronous Compensator (STATCOM), and SST applications. Before the introduction of SiC semiconductors, a considerable number of SMs had to be cascaded to reach the desired MV, resulting in low power density, low efficiency, and high control complexity. SiC and GaN switches, on the other hand, overcame these difficulties and enabled MV applications without cascading identical SMs. Numerous MV applications of NPC converters are available in the literature [144]–[146].

The CHB and MMC topologies provide modularity and scalability and are suitable for MV and high-power applications. The CHB configuration emerged due to its simple control and modulation requirements [147], [148], and minimized THD at the cost of a large coupling inductor [149], [150]. Modularity in MMC and CHB is obtained by connecting identical SMs in series. Both CHB and MMC have common features like fault-tolerant and multilevel operation capabilities with reduced filter size [151]. However, CHB requires an isolated DC supply or a specialized transformer with multiple secondary windings, one per SM, making it less suitable for AC/DC applications or direct interconnection as a rectifier with the grid. Implementing large coupling inductance at a high power level is challenging.

On the other hand, MMC does not require isolated AC or DC supplies and can be directly interconnected with the grid either as a rectifier or inverter. Each SM has an HB structure in MMC consisting of one capacitor and two active switches. The capacitor acts as the DC-link capacitor just like the 2 L converter but is evenly distributed throughout the MMC structure. FB and other specialized SM structures for specific applications can be found in [152], [153]. However,

TABLE 6 A Comparison of MV Front-End Converters for SST.

| MV AFE	Merits	Demerits	Application	Active & Passive Components				Modularity
				Semiconductor	Inductor	Capacitor	Transformer	
NPC	Simple control, DC-link, high power density	Higher voltage switching, bulky filter, low power quality	MV	Maximum	Minimum	Minimum	Minimum	No
CHB	Simple control, low frequency operation for each SM	No DC-link, isolated supplies for each SM	MV	Minimum	Minimum	Moderate	Maximum	Yes
MMC	DC-link, low frequency operation for each SM	Complex control, Bulky capacitors	MV/HV	Minimum	Maximum	Maximum	Maximum	Yes
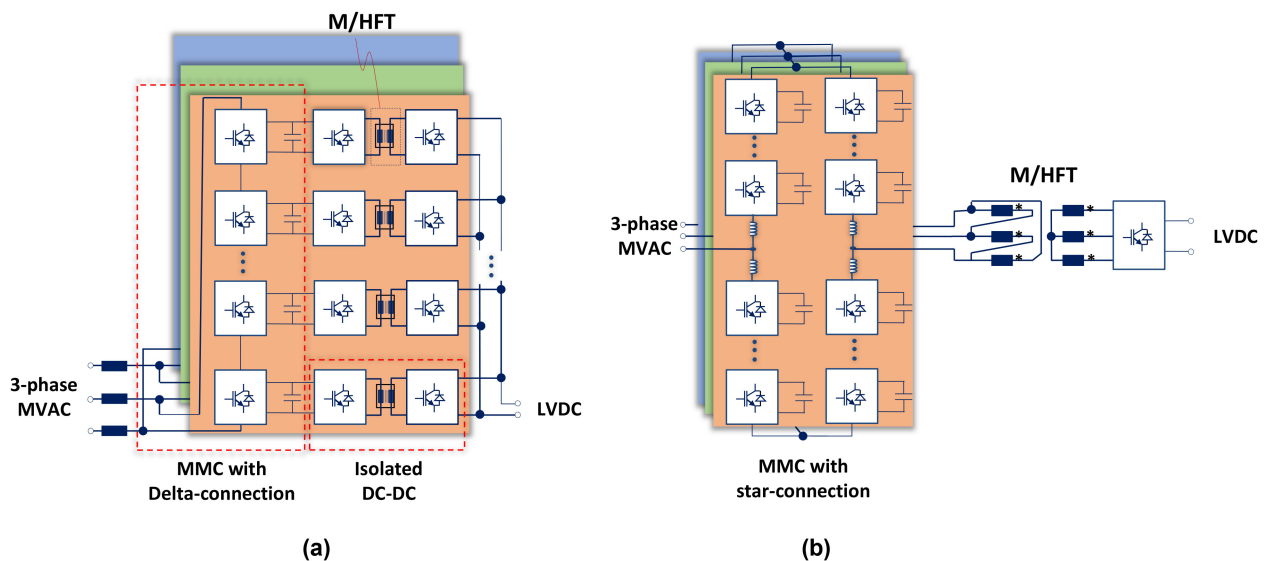
FIGURE 18. MV front-end converters. (a) Delta-connected MMC topology. (b) Star-connected MMC topology.

MMC has a complex control structure and requires a large capacitor on the MVDC side, increasing the total cost of MMC considerably [154]. Delta and star configurations of MMC as front-end are illustrated in Fig. 18(a) and (b), respectively.

Moreover, Fig. 18(a) shows a modular approach of the DC/DC isolation stage as well in which a DC/DC converter follows each MMC SM. On the other hand, Fig. 18(b) depicts the standard approach of isolated DC/DC converters. In addition, to handle high input voltage and provide high output current at the LVDC level, Section VIII-B presents the possible topologies and approaches of back-end DC/DC converters.

B. BACK-END DC/DC CONVERTERS

After an AC/DC conversion stage, a DC/DC converter is required to regulate the instantaneous DC voltage to the desired DC bus voltage and interconnect the RESs, ESSs, and EVs to the common DC bus. Since an EV's battery must not be grounded all the time, as per IEEE Standards 1547, galvanic isolation is required to ensure that battery protection remains unaffected during the charging process. In the UFCS architectures, as shown in Fig. 9, an isolated DC/DC converter is required to provide isolation via an M/HFT located inside the DC/DC converter. In the literature, numerous isolated DC/DC converters with and without PFC capabilities have been extensively researched, and some of the most suitable topologies for UFCS applications are:

One of the viable solutions for unidirectional DC/DC conversion is the PS full-bridge (PSFB) converter, as shown in Fig. 19(a). ZVS is the turn-on condition for this converter that can be achieved with PS PWM. However, this topology suffers from turn-off losses in primary-side active switches, high
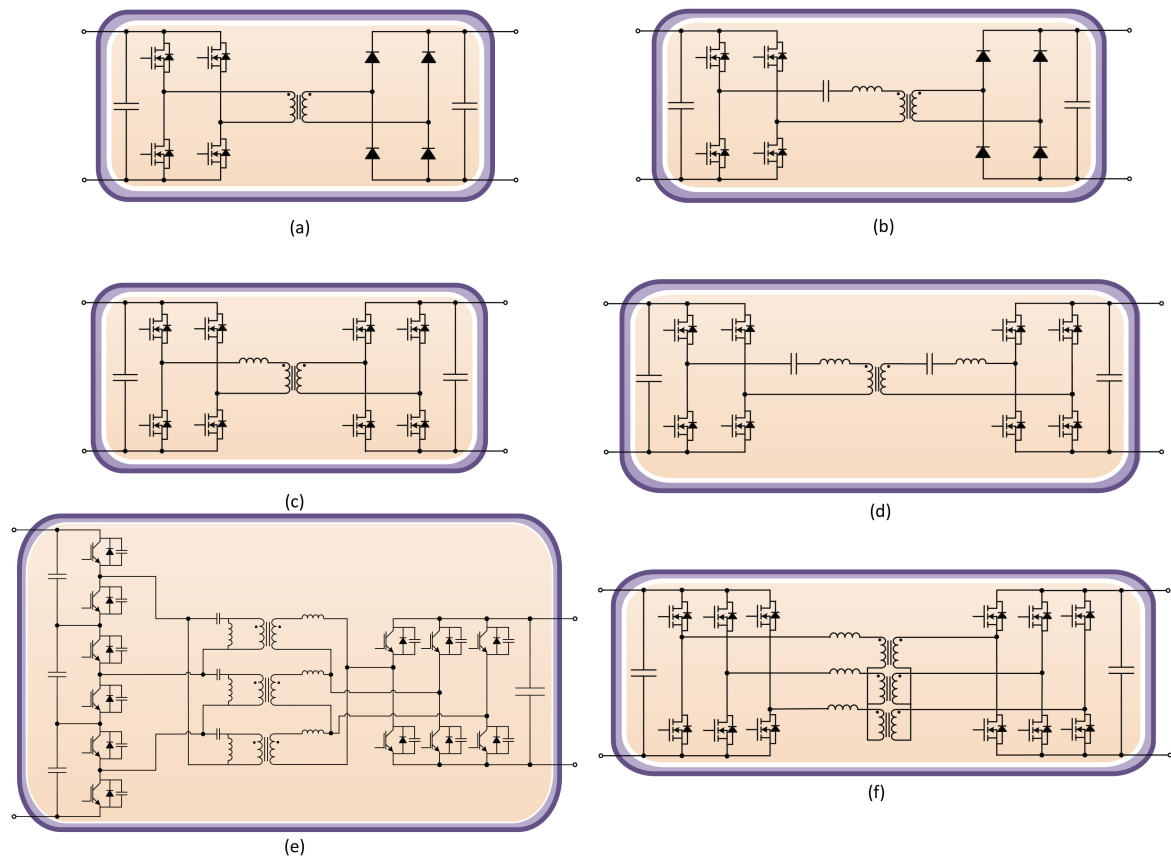
FIGURE 19. Isolated DC/DC converters. (a) PSFB topology. (b) LLC topology. (c) DAB topology. (d) CLLC topology. (e) T^2-LLC topology [173]. (f) 3-ϕ BAD topology.

losses in secondary-side diodes, significant ringing induced by M/HFT leakage inductance, the parasitic capacitance of reverse biased diodes and the output inductor. It has trade-offs between conversion efficiency and voltage overshoot and ringing, as the use of active [155] or passive [156] snubber circuits mitigates the overshoot and ringing issues at the cost of compromised efficiency.

LLC resonant topology, as shown in Fig. 19(b), is another possibility in unidirectional isolated DC/DC converters. In this topology, the output voltage is regulated by varying the switching frequency to match the resonant tank impendence ratio to an equivalent load regulating. The LLC converter achieves ZVS by using magnetizing current, resulting in a minimal turn-off and transformer losses [157], and has high conversion efficiency for a narrow input-to-output voltage ratio [158]. However, it has poor power regulation capabilities in the presence of light load and is unable to sustain ZVS state, and high conversion efficiency over a wide operating range [159]. Furthermore, the component selection is quite difficult due to the high voltage and power stresses on the resonant capacitor. Multilevel LLC [160], parallel modules LLC [161], and 3-ϕ LLC [162] have been proposed in the literature to reduce voltage and power stresses and improve power rating.

A dual active bridge (DAB) converter, as shown in Fig. 19(c), has received much attention for EV charging

applications. It is a good choice for DC/DC conversion because of its inherent galvanic isolation, high power density, bidirectional capability with good efficiency, low device stress, and minimal filter components; it is a good choice for DC/DC conversion. Recently, wide bandgap semiconductor devices such as SiC and GaN, as well as advanced magnetic materials, have contributed significantly to increased interest in the DAB converter [163]. In a DAB, the power flow between the two bridges is similar to the power flow between two voltage buses in a power system. The leakage inductance acts as a power transfer element and regulates the DAB power flow. Due to its simple design and ZVS operation, the DAB converter has been extensively used in isolated bidirectional DC/DC conversion applications [164]. However, the charging profile of EVs requires the converter to operate within a broad range of voltage and power gains, which results in increased reactive power requirements and impaired ZVS operation as well as efficiency [165]. Reactive power and efficiency trade-offs challenge leakage inductance design since a greater inductance permits a broader range of ZVS operation at the expense of reactive power, and vice versa [166]. To tackle this issue, various modulation strategies have been proposed, ranging from a single PS to a dual PS [167] or even a triple PS [168], to increase performance across a broad operating range.
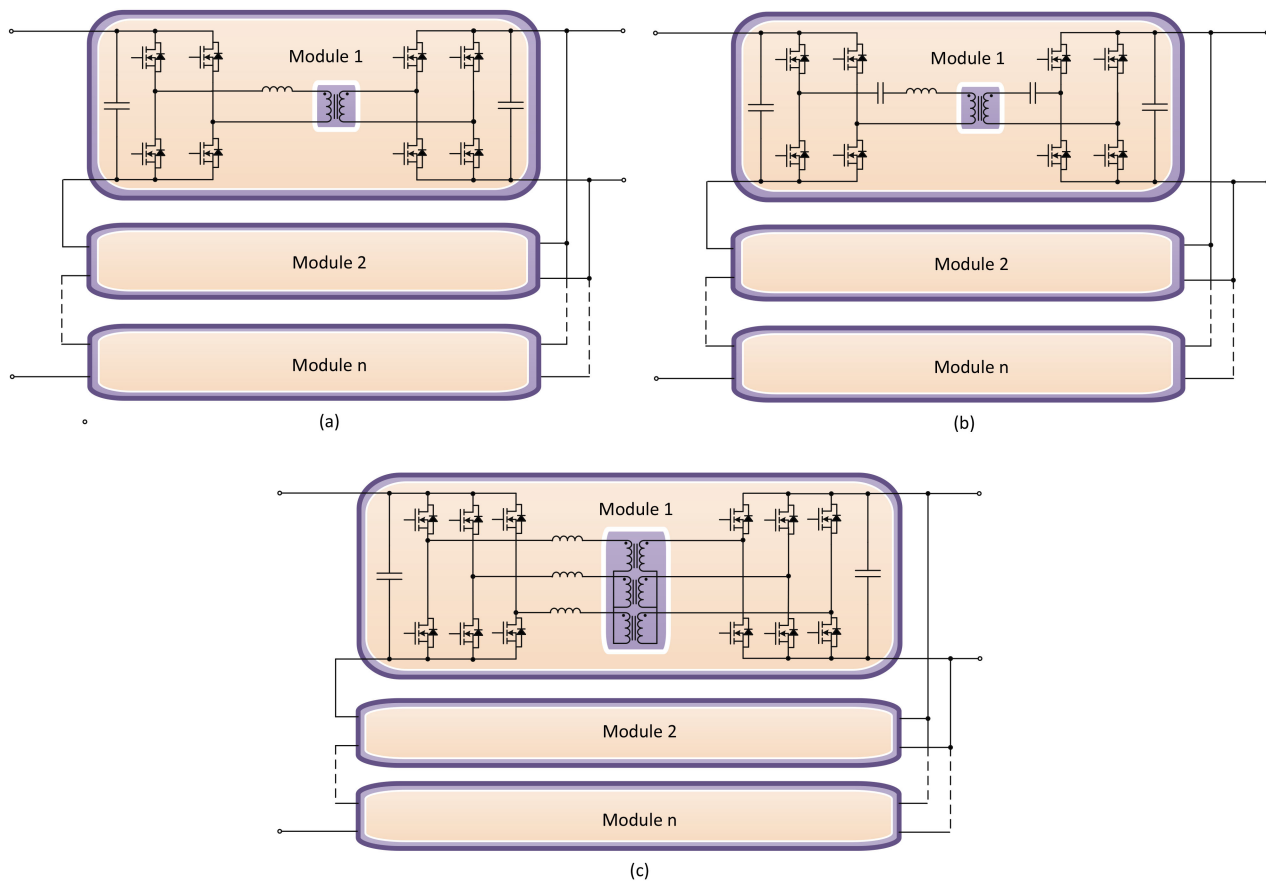
FIGURE 20. Input-series and output-parallel connections of multiple identical modules for MV applications. (a) DAB topology. (b) CLLC topology. (c) 3-ϕ DAB topology.
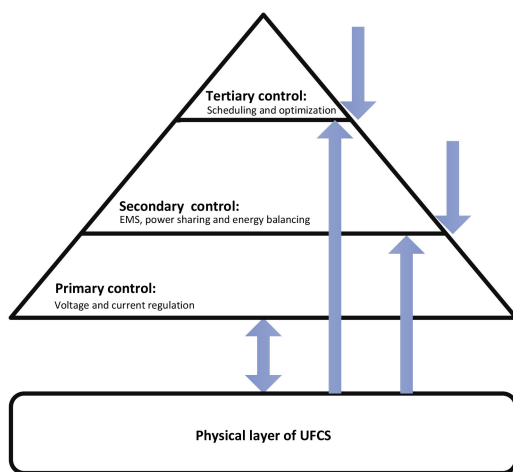

FIGURE 21. A block diagram of the hierarchical control structure.

As shown in Fig. 19(d), CLLC [169] is another important candidate in bidirectional isolated DC/DC converters. The symmetrical structure on both sides enables the converter to provide the same voltage gain with simplified control and better regulation in both directions. In contrast to the LLC topology, the inclusion of capacitors on both sides of M/HFT

minimizes the voltage stress on resonant capacitors [170]. The required leakage inductance for the CLLC resonant tank is substantially smaller than the DAB topology, and so is the amount of reactive power that circulates in the converter, as the sinusoidal resonant current puts less stress on the M/HFT than the DAB converter's [171]. Like DAB, CLLC has also shown certain design trade-offs, such as compromised ZVS and efficiency over a wide voltage and power range. Additionally, due to the steady voltage gain versus frequency curve for a certain range of frequencies, the controllability of the CLLC topology becomes challenging [172].

Three-phase triple-voltage LLC (T^2-LLC) is a new bidirectional resonant converter as shown in Fig. 19(e), is presented in [173]. The proposed converter employs a novel series connection at the input to handle MV and a parallel arrangement at the LVDC side to provide a high current. It can be used as an SM at the DC/DC stage in the SST and has three times more voltage handling capabilities than a traditional resonant converter. However, the efficiency and voltage conversion ratio are sensitive to resonant parameter selection, and the consistency of three-phase resonant parameters must be ensured to achieve a three-phase symmetrical operation. The proposed T^2-LLC converter's primary goals are high efficiency and a fixed voltage conversion ratio. Moreover, an open-loop
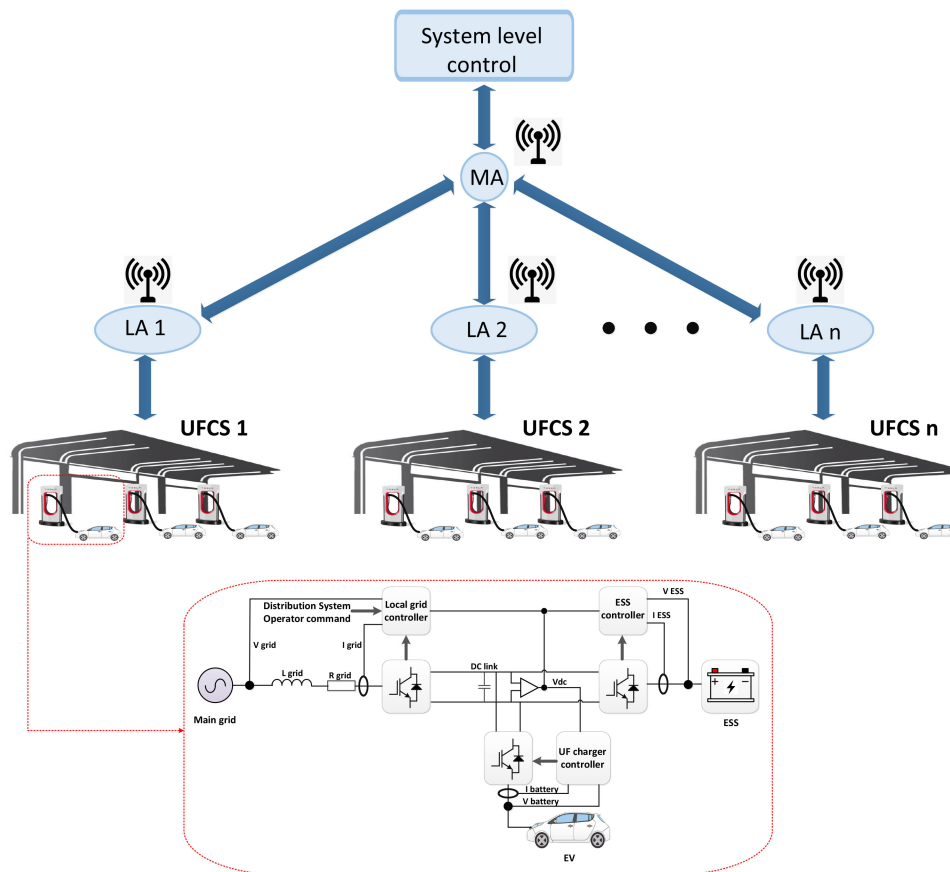
FIGURE 22. An overview of the hierarchical control implementation for UFCSs [189].

control strategy has been used to reduce control complexity and improve the converter design and operation.

Apart from the above topologies, an alternate option is a 3-ϕ BAD, as shown in Fig. 19(f). The operating principles of the 3-ϕ and 1-ϕ BADs are similar. However, unlike the 1-ϕ DAB, the load current is divided into three identical phases connected to three independent M/HFTs. Each M/HFT is designed for only one-third of the converter power rating.

Additionally, the half-bridge (HB) LLC and dual HB (DHB) topologies may be utilized to minimize the number of active switches since the HB topology only has two active switches on each side, which can reduce the converter's cost and losses [174], [175]. Unlike the full-bridge (FB) design, the applied voltage is half of the DC-link voltage, advantageous for M/HFT design. However, the current stress in the HB topologies becomes double and complicates the converter's control.

1) MV BACK-END DC/DC CONVERTERS

The suitable isolated back-end DC/DC converters are covered above and presented in Fig. 19. However, the presence of MV at the input and the high current requirement at the output necessitates the series connection at the MVDC side and the parallel connection at the LVDC side to achieve the required voltage and current ratings. Fig. 20 depicts the modular

versions of Fig. 19(c), (d), and (e) required for MV applications, which not only ensure modularity at the DC/DC stage but also improve a UFCS's fault-tolerant operation. Besides that, the specialized DC/DC topology, i.e., T^2-LLC as shown in Fig. 19(e), can also be used directly for MVDC/LVDC applications.

C. M/HFTS BASED MV/LV ISOLATION

Traditionally, the MV/LV isolation is handled by LFT solutions; however, the demand for high power density and to reduce the use of highly volatile materials such as copper and iron forces to look for M/HFT based SST solutions. Due to the insulation and thermal requirements and other aspects, the higher operating frequency is not always better and applicable. With the high operating frequency, the conduction loss increases due to skin effects, and the thermal limit for the transformer restricts the minimum achievable volume. In terms of the efficiency and power density of the transformer, a smaller number of transformers in the system leads to better performance. In contrast, the optimized frequency limit for the transformer could be set based on the material choice and cooling techniques as per [185]. In modular concepts with several MV isolations, the insulation occupies a significant amount of space; as a result, a centralized transformer has better power density and efficiency. However, mega-watt

TABLE 7 Technical Specifications of Previously Reported M/HFT Prototypes.

Publisher/ Manufacturer	Switching frequency (kHz)	Power rating ((kVA)	Core material	Winding material	Cooling technique	Year
Bombardier [176]	8	500		Solid Cu	Water	2007
FAU [177]	5.6	450		Al	Oil	2011
ETH [178]	20	166	Nanocrystalline		Water	2013
ABB [179]	1.75	150		Litz wire		2014
FREEDM [180]	10	35			Oil	2015
GE [181]	5	1000		Solid Cu		2016
GE [182]	200	50	Ferrite			2018
EPFL [182]	100	100	Si Ferrite	Litz wire		2019
ETH [183]	48	25	Ferrite		Air	
Delta [132]	100 - 200	16				
RWTH [184]	1	5000	Si Steel	Solid Cu		2020

level M/HFT is seldom used due to practical limitations and associated costs of core materials. Table 7 shows the main specifications of previously reported M/HFT prototypes.

IX. UFCS CONTROL

Obviously, a UFCS network that replicates the existing fossil fuel refilling network is required to facilitate a smooth transition towards e-mobility. However, the natures of ICE vehicles' and EVs' refilling networks are diametrically opposite; the former is based on on-site storage and a distribution network to manage supply and demand, whereas the latter requires real-time interconnection with the electricity network and can cause catastrophic failures of the power system in the absence of proper control and management strategies.

A UFCS with integrated RESs and ESS can play a critical role as a point of coupling between the utility grid and distributed resources. Robust control and management strategies are required for realistic models of UFCSs to ensure stable operation in both islanded and grid-connected modes and improve power system stability and reliability. In this regard, the hierarchical control structure of microgrids has been examined for UFCS applications. The control diagram, as illustrated in Fig. 21, consists of three control steps with specified objectives: 1) Voltage and current regulation. 2) An EMS to balance supply and demand. 3) load scheduling to optimize the overall operation of the power system. The implementation of the hierarchical control structure for UFCSs is illustrated in Fig. 22.

A. PRIMARY CONTROL SYSTEM

A primary control system is the basic and silent sentinel required for the stable operation of any dynamic system. In the context of a UFCS, it has to regulate the input and output of each power electronics converter. It is governed by the EMS of the level two-layer via reference signals. It is executed either by current and voltage droop controllers, proportional-integral (PI) controllers, model predictive controllers (MPC), or other nonlinear controllers.

Furthermore, it can be implemented either in a centralized or decentralized fashion. A centralized approach is implemented in [186], where a central controller regulates the front-end AC/DC converter output to guarantee a stable DC bus voltage, and each connected source and load operate in constant power mode. The grid-connected converter requires a dual-loop control structure with inner and outer loops for current and voltage regulation. A PI controller-based dual-loop control system is presented in [187]. Similarly, [188] presents an MPC-based dual-loop control structure to have a stable operation in both grid-connected and islanded modes. The load current is measured and transmitted to a central controller in the proposed approach. Based on the available energy from the grid, RESs and ESSs switching vectors are generated and sent to the converters. At the same time, the voltage loop simultaneously controls the DC bus voltage. Decentralized controllers are getting more attention due to their easy implementation, better controllability, and reliability; they are normally implemented via droop controllers due to their satisfactory performance.

B. SECONDARY CONTROL SYSTEM

Secondary level control, also known as EMS, has the main function of generating reference signals for the primary controllers according to the data received from the tertiary controller. It usually consists of optimization algorithms for profit maximization while satisfying both grid and UFCS constraints. EVs, ESSs, RESs generation, and real-time electricity prices are the main elements involved and related to secondary level control in optimizing a UFCS's operational expenses.

Heuristic methods were traditionally used to predefine the bidirectional power flow between the grid and a UFCS, considering forecasted load demand, RES generation, and the hourly electricity tariff. However, the dynamic tariff, the intermittent nature of RESs, and the unpredictable arrival times of EVs exacerbate optimization challenges. The use of simple heuristic algorithms may result in sub-optimal solutions. [190] proposes a Lagrangian relaxation approach with the optimization goal of increasing the utilization of RESs for ESSs and EV charging. [191] investigated linear programming-based optimization strategies for multiple EV charging in a UFCS. PV generation forecasts are used to maximize RES generation and minimize operational charges. Moreover, a mixed-integer LP is used to study the coordinated charging of EVs with V2G ancillary services for peak shaving, valley filling [192] and frequency regulation.

Recent trends indicate that the primary goals in UFCS research are operational expense minimization as well as

RES and ESS utilization maximization. On the other hand, a coordinated control technique is required to account for the fluctuating nature of RES, the arrival of EVs, weather information, forecasted demand and supply, and other nonlinearities to develop a more beneficial EMS for utility and UFCS operators.

C. TERTIARY CONTROL SYSTEM

Tertiary control is the topmost layer of the control and management structure related to the utility grid. Its main function is to manage the optimal operation of the power system by collecting and sharing real-time supply and demand as well as frequency and voltage conditions with UFCSs. It generates reference signals for the secondary control layer, aiming at the stable and reliable operation of the power system with optimal power flow. Although EVs act both as loads and as sources during charging and discharging processes, they can significantly provide supporting services to power systems. On the other hand, the scheduling of EVs is a complex process. It depends on an EV's power demand, driving patterns, battery characteristics, the number of EVs and UFCSs, and control mechanisms. The control strategy can be implemented either as a centralized or decentralized control structure [193]–[195].

A centralized approach consists of a main aggregator (MA) at the utility level, a local aggregator (LA) at the UFCS level, and a database. Each EV shares its SOC, battery capacity, and required charging power upon arrival; after collecting information, the LA processes and transmits the required power demand to the MA. Based on supply and demand conditions and system parameters and constraints, the MA decides the power allocation for each UFCS. Once the demand is approved, the LA generates the charging points (CPs) command to initiate the charging process. However, after the arrival of EVs, the sharing and processing of information can cause a significant delay. Since the arrival of EVs is unexpected, a database is maintained to request and schedule the daily load in advance by using historical data [196].

On the other hand, the decentralized approach eliminates the need for a LA. EVs are equipped with state-of-the-art ITS devices to communicate with the MA directly. The MA directs an EV towards a UFCS with a free charging slot and stable grid operation after receiving and analyzing the shared information (i.e., SOC, battery capacity, and required charging power). The main benefits of the decentralized approach are adaptability and minimum time delay in guiding EVs towards an optimal UFCS. The parameters, constraints, and objective functions are spread over a broad spectrum. They can cause various optimization problems, there is no single mathematical formulation, and each problem should be tackled according to the real-time information [197].

X. CONCLUSION

Regardless of the exponential increase in the number of on-road EVs and their environmental benefits, the absence of an adequate charging infrastructure to provide rapid and reliable charging facilities during long trips poses challenges to the smooth operation of EVs. To address this issue without compromising the power system's stability and reliability due to the unexpected arrival and impulsive charging demands of EVs, UFCSs with integrated RESs and ESSs having flat load curves and minimal operational expenses are the need of the hour.

The standard AC bus design is adopted by state-of-the-art UFCSs due to mature AC/DC rectifier technology, well-established standards for AC distribution systems, separately developed standards for AC bus UFCSs, and standardized protection methods. In addition to EVs' DC power requirements, the inherent DC nature of RESs and ESSs increases the number of conversion stages in the AC bus architecture and reduces efficiency. On the other hand, standard DC bus design minimizes the conversion stages due to one central AC/DC at the front-end with simple control improved efficiency. It enables the use of partial power converters. Although no standards for DC systems' coordinated control have been developed yet, at a voltage level below 1 kV, DC bus architecture can comply with the AC standards. Suitable power electronics converters for AC and DC bus designs are presented and compared. The charging profile of EVs requires a converter to operate within a broad range of voltage and power gains while providing high efficiency and high power density.

A 350 kW DC UF charger shortens the recharging duration to 10 minutes, which is comparable to the refueling experience of gasoline vehicles. However, because of the associated high power demands, increased capital investment, and MV-grid connection, installing a single UF charger is prohibitively expensive. In contrast, a UFCS with multiple chargers makes more economic sense than a single-port charger. The high power demand for UF charging means the UFCS acts as a massive load center for the power system, and integrated RESs and ESSs not only normalized the power demand and reduced the operational expenses of the UFCSs significantly but also enabled UFCSs to provide ancillary grid services such as voltage and frequency support services.

The replacement of the LFT with the SST provides the voltage step-down, conversion, and isolation with several unique features, such as fault current limitations, fault isolation, improved convertibility, better controllability, reduced footprint, higher efficiency at light load, modularity, fault-tolerant structure, and bidirectional power flow.

However, SST technology is still at the research and development phase and has not matured yet. Some of the common concerns and deficiencies that must be addressed are as follows:

- The use of SS devices significantly reduces the weight and size of SST, but it also increases the price of SST many times more than LFT. As a result, the use of LV SS devices with low losses and HF operation characteristics can help to reduce the required heat sinks and passive components, contributing to the overall cost reduction of SST. Similarly, the use of wide-bandgap devices such

as SiC and GaN can help to reduce the number of SS devices and their corresponding heat sinks.

- Although SST offers high power density, it suffers from efficiency and reliability issues. Most of the MV and HV applications are currently realized by modular SSTs, which results in high cost and power quality concerns. The single-cell SST is a promising approach, but it experiences reliability concerns due to its non-modular structure.

- A robust control and protection mechanism is the key performance indicator of SST. Due to the limited in-built overvoltage and overcurrent protection schemes, SST's protection reliability is lower than LFT. To compensate for this drawback, external protection devices compromised the weight and size of the SST. The use of SS protection devices, on the other hand, requires a less robust control structure, but it is still far away from practical implementation at the MV level.

- Real-time data exchange between the SST and the grid station is required for advanced protection schemes. As a result, communication systems that satisfy the latency, security, and reliability requirements need to be selected appropriately.

REFERENCES

[1] S. Rezaee, E. Farjah, and B. Khorramdel, "Probabilistic analysis of plug-in electric vehicles impact on electrical grid through homes and parking lots," *IEEE Trans. Sustain. Energy*, vol. 4, no. 4, pp. 1024–1033, Oct. 2013.

[2] The Paris Agreement-UNFCCC, Accessed: Jun. 13, 2022. [Online]. Available: https://unfccc.int/sites/default/files/resource/parisagreement_publication.pdf

[3] M. F. M. Sabri, K. A. Danapalasingam, and M. F. Rahmat, "A review on hybrid electric vehicles architecture and energy management strategies," *Renewable Sustain. Energy Rev.*, vol. 53, pp. 1433–1442, Jan. 2016.

[4] J. Larminie and J. Lowry, *Electric Vehicle Technology Explained*. New York, NY, USA: Wiley, 2003.

[5] EV30@30 Campaign. Accessed: Jun. 13, 2022. [Online]. Available: https://iea.blob.core.windows.net/assets/8cbeac6e-50e5-4a50-909c-24108adaf603/CampaignDocumentupdate_2020.pdf

[6] "Global commercial vehicle drive to zero campaign," Accessed: Jun. 13, 2022. [Online]. Available: [Online]. Available: https://globaldrivetozero.org/

[7] Environment Facility (GEF), Accessed: Jun. 13, 2022. [Online]. Available: https://www.thegef.org/

[8] K. Lebeau, J. van Mierlo, P. Lebeau, O. Mairesse, and C. Macharis, "Consumer attitudes towards battery electric vehicles: A large-scale survey," *Int. J. Electric Hybrid Veh.*, vol. 5, no. 1, pp. 28–41, Apr. 2013.

[9] S. Manzetti and F. Mariasiu, "Electric vehicle battery technologies: From present state to future systems," *Renewable Sustain. Energy Rev.*, vol. 51, pp. 1004–1012, Nov. 2015.

[10] B. Marmiroli, M. Messagie, G. Dotelli, and J. Van Mierlo, "Electricity generation in LCA of electric vehicles: A review," *Appl. Sci.*, vol. 8, no. 8, Aug. 2018, Art. no. 1384.

[11] K. Edström, "BATTERY 2030+. Inventing the Sustainable Batteries of the Future. Research Needs and Future Actions," Accessed: Jun. 13, 2022. [Online]. Available: https://battery2030.eu/digitalAssets/860/c_860904-l_1-k_roadmap-27-march.pdf

[12] M. A. Hannan, M. M. Hoque, A. Hussain, Y. Yusof, and P. J. Ker, "State-of-the-art and energy management system of lithium-ion batteries in electric vehicle applications: Issues and recommendations," *IEEE Access*, vol. 6, pp. 19362–19378, 2018.

[13] J. Y. Yong, V. K. Ramachandaramurthy, K. M. Tan, and N. Mithulananthan, "A review on the state-of-the-art technologies of electric vehicle, its impacts and prospects," *Renewable Sustain. Energy Rev.*, vol. 49, pp. 365–385, Oct. 2015.

[14] N. Keshmiri, D. Wang, B. Agrawal, R. Hou, and A. Emadi, "Current status and future trends of GaN HEMTs in electrified transportation," *IEEE Access*, vol. 8, pp. 70553–70571, 2020.

[15] P. P. G. Microsemi, "Gallium Nitride (GaN) versus Silicon Carbide (SiC) in the High Frequency (RF) and power switching applications," Accessed: Jun. 13, 2022. [Online]. Available: https://www.richardsonrfpd.com/docs/rfpd/Microsemi-A-Comparison-of-Gallium-Nitride-Versus-Silicon-Carbide.pdf

[16] J. V. Mierlo *et al.*, "Beyond the state of the art of electric vehicles: A fact-based paper of the current and prospective electric vehicle technologies," *World Electric Veh. J.*, vol. 12, no. 1, pp. 20, Feb. 2021.

[17] H. Rasool, M. El Baghdadi, A. Manan Rauf, A. Zhaksylyk, and O. Hegazy, "A rapid non-linear computation model of power loss and electro thermal behaviour of three-phase inverters in EV drivetrains," in *Proc. Int. Symp. Power Electron. Elect. Drives Automat. Motion*, 2020, pp. 317–323.

[18] D. D. Tran, M. Vafaeipour, M. Baghdadi, R. Barrero, J. van Mierlo, and O. Hegazy, "Thorough state-of-the-art analysis of electric and hybrid vehicle powertrains: Topologies and integrated energy management strategies," *Renewable Sustain. Energy Rev.*, vol. 119, Mar. 2020, Art. no. 109596.

[19] E. S. Islam, A. Moawad, N. Kim, and A. Rousseau, "Vehicle electrification impacts on energy consumption for different connected-autonomous vehicle scenario runs," *World Electric Veh. J.*, vol. 11, no. 1, Dec. 2019, Art. no. 9.

[20] IEA, "Global EV Outlook 2021, IEA, Paris," 2021. Accessed: Jun. 13, 2022. [Online]. Available: https://www.iea.org/reports/global-ev-outlook-2021

[21] IEA, "Global electric vehicle stock by region," 2010-2020, IEA, Paris. Accessed: Jun. 13, 2022. [Online]. Available: https://www.iea.org/data-and-statistics/charts/global-electric-vehicle-stock-by-region-2010-2020

[22] IEA, "Consumer and government spending on electric cars," 2015-2020, IEA, Paris. Accessed: Jun. 13, 2022. [Online]. Available: https://www.iea.org/data-and-statistics/charts/consumer-and-government-spending-on-electric-cars-2015-2020

[23] IEA, "National subsidies for EV purchase before and after economic stimulus measures," 2020, IEA, Paris. Accessed: Jun. 13, 2022. [Online]. Available: https://www.iea.org/data-and-statistics/charts/national-subsidies-for-ev-purchase-before-and-after-economic-stimulus-measures-2020

[24] M. Li, J. Lu, Z. Chen, and K. Amine, "30 years of lithium-ion batteries," *Adv. Mater.*, vol. 30, 2018, Art. no. 1800561.

[25] R. Schmuch, R. Wagner, G. Hörpel, T. Placke, and M. Winter, "Performance and cost of materials for lithium-based rechargeable automotive batteries," *Nature Energy*, vol. 3, pp. 267–278, Apr. 2018.

[26] R. Gopalakrishnan, *et al.*, "A comprehensive study on rechargeable energy storage technologies," *J. Electrochem. En. Conv. Stor.*, vol. 13, no. 4, pp. 1-25, Apr. 2016.

[27] J. Xie and Y. C. Lu, "A retrospective on lithium-ion batteries," *Nature Commun.*, vol. 11, pp. 1–4, 2020.

[28] M. Philippot, G. Alvarez, E. Ayerbe, J. van Mierlo, and M. Messagie, "Eco-efficiency of a lithium-ion battery for electric vehicles: Influence of manufacturing country and commodity prices on GHG emissions and costs," *Batteries*, vol. 5, no. 1, Feb. 2019, Art. no. 23.

[29] G. Berckmans *et al.*, "Analysis of the effect of applying external mechanical pressure on next generation silicon alloy lithium-ion cells," *Electrochimica Acta*, vol. 306, pp. 387–395, May 2019.

[30] P. Albertus, S. Babinec, S. Litzelman, and A. Newman, "Status and challenges in enabling the lithium metal electrode for high-energy and low-cost rechargeable batteries," *Nature Energy*, vol. 3, pp. 16–21, Dec. 2017.

[31] M. Pasta *et al.*, "2020 roadmap on solid-state batteries," *J. Phys. Energy*, vol. 2, Aug. 2020, Art. no. 032008.

[32] S. Randau *et al.*, "Benchmarking the performance of all-solid-state lithium batteries," *Nature Energy*, vol. 5, pp. 259–270, Mar. 2020.

[33] IEA, "Stock of slow public electric light duty vehicles chargers," 2015-2020, IEA, Paris. Accessed: Jun. 13, 2022. [Online]. https://www.iea.org/data-and-statistics/charts/stock-of-slow-public-electric-light-duty-vehicles-chargers-2015-2020

[34] IEA, "Stock of fast public electric light duty vehicles chargers," 2015-2020, IEA, Paris. Accessed: Jun. 13, 2022. [Online]. https://www.iea.org/data-and-statistics/charts/stock-of-fast-public-electric-light-duty-vehicles-chargers-2015-2020

[35] "Directive 2014/94/EU of the European Parliament and of the Council of the deployment of alternative fuels infrastructure with EEA relevance," Oct. 22, 2014. Accessed: Jun. 13, 2022. [Online]. Available: http://data.europa.eu/eli/dir/2014/94/oj

[36] C. Botsford and A. Szczepanek, "Fast charging vs. slow charging: Pros and cons for the new age of electric vehicles," in *Proc. Int. Battery Hybrid Fuel Cell Electric Veh. Symp.*, 2009, pp. 1–9.

[37] R. Wolbertus and R. van den Hoed, "Fast charging systems for passenger electric vehicles," *World Electric Veh. J.*, vol. 11, no. 4, Nov. 2020, Art. no. 73.

[38] *IEEE Application Guide for IEEE Std 1547TM, IEEE Standard for Interconnecting Distributed Resources With Electric Power Systems*, IEEE Standard 1547.2-2008, 2009.

[39] H. Tu, H. Feng, S. Srdic, and S. Lukic, "Extreme fast charging of electric vehicles: A technology overview," *IEEE Trans. Trans. Electrific.*, vol. 5, no. 4, pp. 861–878, Dec. 2019.

[40] E. Loveday, "Rare look inside tesla supercharger," Accessed: Jun. 13, 2022. [Online]. Available: https://insideevs.com/news/322486/rare-look-inside-tesla-supercharger/

[41] *SAE Electric Vehicle and Plug in Hybrid Electric Vehicle Conductive Charge Coupler*, Standard SAE J1772, Oct. 2017.

[42] T. S. Ustun, C. R. Ozansoy, and A. Zayegh, "Implementing vehicle-togrid (V2G) technology with IEC 61850-7-420," *IEEE Trans. Smart Grid*, vol. 4, no. 2, pp. 1180–1187, Jun. 2013.

[43] A. Yoshida, "Chademo quick charger connector with excellent operability," Accessed: Jun. 13, 2022. [Online]. Available: https://globalsei.com/technology/tr/bn84/pdf/84-05.pdf

[44] L. Wang, Z. Qin, T. Slangen, P. Bauer, and T. van Wijk, "Grid impact of electric vehicle fast charging stations: Trends, standards, issues and mitigation measures - an overview," *IEEE Open J. Power Electron.*, vol. 2, pp. 56–74, Jan. 2021.

[45] Occupational Safety and Health Administration, "OSHA lifting limit," Accessed: Jun. 13, 2022. [Online]. Available: https://www.cdc.gov/niosh/docs/94-110/pdfs/94-110revised082021.pdf?id=10.26616/NIOSHPUB94110

[46] A. Burnham *et al.*, "Enabling fast charging–infrastructure and economic considerations," *J. Power Sources*, vol. 367, pp. 237–249, Nov. 2017.

[47] M. Smith and J. Castellano, "Costs associated with non-residential electric vehicle supply equipment: Factors to consider in the implementation of electric vehicle charging stations," New West Technol., LLC, Portland, OR, USA, Tech. Rep. DOE/EE-1289, 2015.

[48] Z. Xu, Z. Hu, Y. Song, Z. Luo, K. Zhan, and J. Wu, "Coordinated charging strategy for PEVs charging stations," in *Proc. IEEE Power Energy Soc. Gen. Meeting*, 2012, pp. 1–8.

[49] M. Tabari and A. Yazdani, "An energy management strategy for a DC distribution system for power system integration of plug-in electric vehicles," *IEEE Trans. Smart Grid*, vol. 7, no. 2, pp. 659–668, Mar. 2016.

[50] E. Veldman and R. A. Verzijlbergh, "Distribution grid impacts of smart electric vehicle charging from different perspectives," *IEEE Trans. Smart Grid*, vol. 6, no. 1, pp. 333–342, Jan. 2015.

[51] R. Abousleiman and R. Scholer, "Smart charging: System design and implementation for interaction between plug-in electric vehicles and the power grid," *IEEE Trans. Transp. Electrific.*, vol. 1, no. 1, pp. 18–25, Jun. 2015.

[52] O. Beaude, S. Lasaulce, M. Hennebel, and I. Mohand-Kaci, "Reducing the impact of EV charging operations on the distribution network," *IEEE Trans. Smart Grid*, vol. 7, no. 6, pp. 2666–2679, Nov. 2016.

[53] B. Sun, Z. Huang, X. Tan, and D. H. K. Tsang, "Optimal scheduling for electric vehicle charging with discrete charging levels in distribution grid," *IEEE Trans. Smart Grid*, vol. 9, no. 2, pp. 624–634, Mar. 2018.

[54] M. H. Mobarak and J. Bauman, "Vehicle-directed smart charging strategies to mitigate the effect of long-range EV charging on distribution transformer aging," *IEEE Trans. Transp. Electrific.*, vol. 5, no. 4, pp. 1097–1111, Dec. 2019.

[55] B. Baatar, K. Heckmann, T. Hoang, R. Jarvis, and P. Sakhiya, "Preparing rural America for the electric vehicle revolution," Univ. California, Davis, CA, USA, Tech. Rep., 2019.

[56] S. Gallinaro, "Energy storage systems boost electric vehicles' fast charger infrastructure," Accessed: Jun. 13, 2022. [Online]. Available: https://www.analog.com/media/en/technicaldocumentation/tech-articles/energy-storage-systems-boosting-theelectric-vehicles-fast-charger-infrastructure.pdf

[57] S. Negarestani, M. Fotuhi-Firuzabad, M. Rastegar, and A. Rajabi-Ghahnavieh, "Optimal sizing of storage system in a fast charging station for plug-in hybrid electric vehicles," *IEEE Trans. Transp. Electrific.*, vol. 2, no. 4, pp. 443–453, Dec. 2016.

[58] F. Koyanagi and Y. Uriu, "A strategy of load leveling by charging and discharging time control of electric vehicles," *IEEE Trans. Power Syst.*, vol. 13, no. 3, pp. 1179–1184, Aug. 1998.

[59] C. D. White and K. M. Zhang, "Using vehicle-to-grid technology for frequency regulation and peak-load reduction," *J. Power Sources*, vol. 196, no. 8, pp. 3972–3980, Apr. 2011.

[60] T. Wu, Q. Yang, Z. Bao, and W. Yan, "Coordinated energy dispatching in microgrid with wind power generation and plug-in electric vehicles," *IEEE Trans. Smart Grid*, vol. 4, no. 3, pp. 1453–1463, Sep. 2013.

[61] M. Kesler, M. C. Kisacikoglu, and L. M. Tolbert, "Vehicle-to-grid reactive power operation using plug-in electric vehicle bidirectional offboard charger," *IEEE Trans. Ind. Electron.*, vol. 61, no. 12, pp. 6778–6784, Dec. 2014.

[62] J. Y. Yong, V. K. Ramachandaramurthy, K. M. Tan, and N. Mithulananthan, "Bi-directional electric vehicle fast charging station with novel reactive power compensation for voltage regulation," *Int. J. Elect. Power Energy Syst.*, vol. 64, pp. 300–310, Jan. 2015.

[63] W. Hu, C. Su, Z. Chen, and B. Bak-Jensen, "Optimal operation of plug-in electric vehicles in power systems with high wind power penetrations," *IEEE Trans. Sustain. Energy*, vol. 4, no. 3, pp. 577–585, Jul. 2013.

[64] M. Ghofrani, A. Arabali, M. Etezadi-Amoli, and M. S. Fadali, "Smart scheduling and cost-benefit analysis of grid-enabled electric vehicles for wind power integration," *IEEE Trans. Smart Grid*, vol. 5, no. 5, pp. 2306–2313, Sep. 2014.

[65] S. Bai, Y. Du, and S. Lukic, "Optimum design of an EV/PHEV charging station with DC bus and storage system," in *Proc. IEEE Energy Convers. Congr. Expo.*, 2010, pp. 1178–1184.

[66] Y. Cao, N. Wang, G. Kamel, and Y.-J. Kim, "An electric vehicle charging management scheme based on publish/subscribe communication framework," *IEEE Syst. J.*, vol. 11, no. 3, pp. 1822–1835, Sep. 2017.

[67] Y. Cao, Y. Miao, G. Min, T. Wang, Z. Zhao, and H. Song, "Vehicular-publish/subscribe (V-P/S) communication enabled on-the move EV charging management," *IEEE Commun. Mag.*, vol. 54, no. 12, pp. 84–92, Dec. 2016.

[68] Intelligent Transport Systems (ITS), "Infrastructure to vehicle communication; Part 1: Electric vehicle charging spot notification specification," Eur. Telecommun. Std. Inst., Sophia-Antipolis Cedex, France, Tech. Rep. ETSI TS101556-1v1.1.1.

[69] Intelligent Transport Systems (ITS), "Infrastructure to vehicle communications; Part 3: Communications system for the planning and reservation of EV energy supply using wireless networks," Eur. Telecommun. Std. Inst., Sophia-Antipolis Cedex, France, Tech. Rep. ETSI TS101556-3v1.1.1.

[70] D. Sbordone, I. Bertini, B. Di Pietra, M. C. Falvo, A. Genovese, and L. Martirano, "EV fast charging stations and energy storage technologies: A real implementation in the smart micro grid paradigm," *Electric Power Syst. Res.*, vol. 120, pp. 96–108, Mar. 2015.

[71] *Electric Vehicle Conductive Charging System Part 23: DC Electric Vehicle Charging Station*, Standard IEC 61851-23,2014, Mar. 2014, pp. 1–159.

[72] *Electric Vehicle Conductive Charging System–Part 1: General Requirements*, Standard IEC 61851-1:2017, 2017.

[73] *Electric Vehicle Conductive Charging System–Part 24: Digital Communication Between A. D. C. EV Charging Station and an Electric Vehicle for Control of D. C. Charging*, Standard IEC 61851-242014, 2014.

[74] A. Agius, "What's involved in the construction of an ultra-rapid electric car charging station?," Accessed: Jun. 13, 2022. [Online]. Available: https://www.drivezero.com.au/charging/whats-involved-in-the-construction-of-an-ultra-rapidelectric-car-charging-station/

[75] Zekalabs, "Electric buses DC charging stations," Accessed: Jun. 13, 2022. [Online]. Available: https://www.zekalabs.com/applications/electric-buses-dc-charging-stations

[76] S. Bai and S. M. Lukic, "Unified active filter and energy storage system for an MW electric vehicle charging station," *IEEE Trans. Power Electron.*, vol. 28, no. 12, pp. 5793–5803, Dec. 2013.

[77] M. S. Agamy *et al.*, "An efficient partial power processing DC/DC converter for distributed PV architectures," *IEEE Trans. Power Electron.*, vol. 29, no. 2, pp. 674–686, Feb. 2014.

[78] W. Yu, J. Lai, H. Ma, and C. Zheng, "High-efficiency DC-DC converter with twin bus for dimmable led lighting," *IEEE Trans. Power Electron.*, vol. 26, no. 8, pp. 2095–2100, Aug. 2011.

[79] J. Rojas, H. Renaudineau, S. Kouro, and S. Rivera, "Partial power DC-DC converter for electric vehicle fast charging stations," in *Proc. 43rd Annu. Conf. IEEE Ind. Electron. Soc.*, 2017, pp. 5274–5279.

[80] V. Mahadeva Iyer, S. Gulur, G. Gohil, and S. Bhattacharya, "An approach towards extreme fast charging station power delivery for electric vehicles with partial power processing," *IEEE Trans. Ind. Electron.*, vol. 67, no. 10, pp. 8076–8087, Oct. 2020.

[81] P. Purgat, N. H. van der Blij, Z. Qin, and P. Bauer, "Partially rated power flow control converter modeling for low-voltage DC grids," *IEEE J. Emerg. Sel. Topics Power Electron.*, vol. 8, no. 3, pp. 2430–2444, Sep. 2020.

[82] Z. Guo, D. Sha, X. Liao, and J. Luo, "Input-series-output-parallel phase-shift full-bridge derived DC–DC converters with auxiliary LC networks to achieve wide zero-voltage switching range," *IEEE Trans. Power Electron.*, vol. 29, no. 10, pp. 5081–5086, Oct. 2014.

[83] Y. Shi and X. Yang, "Wide range soft switching PWM three-level DC–DC converters suitable for industrial applications," *IEEE Trans. Power Electron.*, vol. 29, no. 2, pp. 603–616, Feb. 2014.

[84] P. Purgat *et al.*, "Design criteria of solid-state circuit breaker for low voltage microgrids," *IET Power Electron*, vol. 14, no. 7, pp. 1284–1299, 2021.

[85] S. Augustine, J. E. Quiroz, M. J. Reno, and S. Brahma, "DC microgrid protection: Review and challenges," *Sandia Nat. Lab.*, Albuquerque, NM, USA, Tech. Rep. SAND2018-8853, 2018.

[86] P. Purgat, A. Shekhar, Z. Qin, and P. Bauer, "Low-voltage dc system building blocks: Integrated power flow control and short circuit protection," *IEEE Trans. Ind. Electron*, to be published, doi: 10.1109/MIE.2021.3106275.

[87] J.-D. Park and J. Candelaria, "Fault detection and isolation in lowvoltage DC-bus microgrid system," *IEEE Trans. Power Del.*, vol. 28, no. 2, pp. 779–787, Apr. 2013.

[88] M. Nicholas and D. Hall, "Lessons learned on early fast electric vehicle charging systems," Int. Council Clean Transp., Washington, DC, USA, Tech. Rep., 2018, Accessed: Jun. 13, 2022. [Online]. Available: https://theicct.org/wp-content/uploads/2021/06/ZEV_fast_charging_white_paper_final.pdf

[89] C. Molnar, "Norway needs $1.6-Billion power grid upgrade to support EVs by 2040: Study driving," Accessed: Jun. 13, 2022. [Online]. Available: https://driving.ca/auto-news/news/norway-needs-1-6-billionpower-grid-upgrade-to-support-evs-by-2040-study

[90] M. A. H. Rafi and J. Bauman, "A comprehensive review of DC fast-charging stations with energy storage: Architectures, power converters, and analysis," *IEEE Trans. Transp. Electrif.*, vol. 7, no. 2, pp. 345–368, Jun. 2021.

[91] S. Knupfer, J. Noffsinger, and S. Sahdev, "How battery storage can help charge the electric-vehicle market. McKinsey & Company," Accessed: Jun. 13, 2022. [Online]. Available: https://www.mckinsey.com/business-functions/sustainability/our-insights/how-battery-storage-can-help-charge-the-electric-vehicle-market

[92] J. McLaren, P. Gagnon, D. Zimny-Schmitt, M. DeMinco, and E. Wilson, "Maximum demand charge rates for commercial and industrial electricity tariffs in the United States," Nat. Renew. Energy Lab., Golden, CO, USA, Tech. Rep. 74, doi: 10.7799/1392982.

[93] DNV (2016), "Battery energy storage systems in the Netherlands, 2016," Accessed: Jun. 13, 2022. [Online]. Available: https://https://www.dnv.com/Publications/battery-energy-storage-systems-in-the-netherlands-203632

[94] M. Zidar, N. D. Hatziargyriou, D. Škrlec, T. Capuder, and P. S. Georgilakis, "Review of energy storage allocation in power distribution networks: Applications, methods and future research," *IET Gener. Transmiss. Distrib.*, vol. 10, no. 3, pp. 645–652, Feb. 2016.

[95] A. Nagarajan and R. Ayyanar, "Design and strategy for the deployment of energy storage systems in a distribution feeder with penetration of renewable resources," *IEEE Trans. Sustain. Energy*, vol. 6, no. 3, pp. 1085–1092, Jul. 2015.

[96] X. Li, L. Yao, and D. Hui, "Optimal control and management of a large-scale battery energy storage system to mitigate fluctuation and intermittence of renewable generations," *J. Modern Power Syst. Clean Energy*, vol. 4, no. 4, pp. 593–603, Oct. 2016.

[97] H. Beltran, E. Bilbao, E. Belenguer, I. Etxeberria-Otadui, and P. Rodriguez, "Evaluation of storage energy requirements for constant production in PV power plants," *IEEE Trans. Ind. Electron.*, vol. 60, no. 3, pp. 1225–1234, Mar. 2013.

[98] A. Colthrope, "Round-Up: 60MWh Japan project, Northern Ireland's 10MW Array and Imergy Goes for Africa Teleco," Accessed: Jun. 13, 2022. [Online]. Available: https://www.energy-storage.news/round-up-60mwh-japan-project-northern-irelands-10mw-array-and-imergy-goes-for-africa-teleco/

[99] A. Ratnayake, "Notrees wind storage project description," Duke Energy. Accessed: Jun. 13, 2022. [Online]. Available: https://www.sandia.gov/ess-ssl/docs/pr_conferences/2011/3_Ratnayake_Notrees.pdf

[100] M. Montoya and K. Nuhfer, "Tehachapi wind energy storage project," U.S. Department of Energy, Accessed: Jun. 13, 2022. [Online]. Available: https://www.energy.gov/sites/prod/files/Tehachapi.pdf

[101] S. Barrett, "E.ON inaugurates first 2 MW power-to-gas unit in Falkenhagen," *Fuel Cells Bulletin*, vol. 2013, no. 9, p. 9, Sep. 2013, doi: 10.1016/S1464-2859(13)70325-0.

[102] D. Gielen, E. Taibi, and R. Miranda, "Hydrogen: A renewable energy perspective," Int. Renew. Energy Agency, Tokyo, Japan, Tech. Rep., Sep. 2019. Accessed: Jun. 13, 2022. [Online]. Available: https://www.h2knowledgecentre.com/content/policypaper1305

[103] M. Blenner and B. Rosen, "EVGO balances EV fast charging with 14 battery storage systems across 11 EVGO fast charging stations," 2009. Accessed: Jun. 13, 2022. [Online]. Available: https://www.evgo.com/about/news/evgobalances-ev-fast-charging-with-14-battery-storage-systems-across-11-evgo-fast-charging-stations/

[104] F. Lambert, "Tesla opens new V3 supercharger with solar and battery-looks like EV charging station of the future. Electrek," 2009. Accessed: Jun. 13, 2022. [Online]. Available: https://electrek.co/2019/07/18/tesla-v3-supercharger-station-las-vegas-solar-power-battery/

[105] F. Lambert, "Aston Martin unveils latest all-electric rapide E prototype with 800V powertrain, Electrek," Accessed: Jun. 13, 2022. [Online]. Available: https://electrek.co/2019/01/25/aston-martin-electric-rapideprototype-800v-powertrain/

[106] M. Wienkötter, "The battery: Sophisticated thermal management, 800-volt system voltage, Porsche," Accessed: Jun. 13, 2022. [Online]. Available: https://newsroom.porsche.com/en/products/taycan/battery-18557.html

[107] X. Yu, X. She, X. Zhou, and A. Q. Huang, "Power management for DC microgrid enabled by solid-state transformer," *IEEE Trans. Smart Grid*, vol. 5, no. 2, pp. 954–965, Mar. 2014.

[108] X. She, A. Q. Huang, S. Lukic, and M. E. Baran, "On integration of solid-state transformer with zonal DC microgrid," *IEEE Trans. Smart Grid*, vol. 3, no. 2, pp. 975–985, Jun. 2012.

[109] X. She, A. Q. Huang, and R. Burgos, "Review of solid-state transformer technologies and their application in power distribution systems," *IEEE J. Emerg. Sel. Topics Power Electron.*, vol. 1, no. 3, pp. 186–198, Sep. 2013.

[110] A. Q. Huang, "Medium-voltage solid-state transformer: Technology for a smarter and resilient grid," *IEEE Ind. Electron. Mag.*, vol. 10, no. 3, pp. 29–42, Sep. 2016.

[111] M. Vasiladiotis and A. Rufer, "A modular multiport power electronic transformer with integrated split battery energy storage for versatile ultrafast EV charging stations," *EEE Trans. Ind. Electron.*, vol. 62, no. 5, pp. 3213–3222, May 2015.

[112] L. S. Xavier, W. C. S. Amorim, A. F. Cupertino, V. F. Mendes, W. C. do Boaventura, and H. A. Pereira, "Power converters for battery energy storage systems connected to medium voltage systems: A comprehensive review," *MC Energy*, vol. 1, no. 1, pp. 1–15, Dec. 2019.

[113] F. Ruiz, M. A. Perez, J. R. Espinosa, T. Gajowik, S. Stynski, and M. Malinowski, "Surveying solid-state transformer structures and controls: Providing highly efficient and controllable power flow in distribution grids," *IEEE Ind. Electron. Mag.*, vol. 14, no. 1, pp. 56–70, Mar. 2020.

[114] J. Wang, A. Q. Huang, W. Sung, Y. Liu, and J. Baliga, "Development of 15-kV SiC IGBTs and their impact on utility applications," *IEEE Ind. Mag.*, vol. 3, no. 2, pp. 16–23, Jun. 2009.

[115] M. Liserre, G. Buticchi, M. Andresen, G. De Carne, L. F. Costa, and Z.-X. Zou, "The smart transformer: Impact on the electric grid and technology challenges," *IEEE Ind. Electron. Mag.*, vol. 10, no. 2, pp. 46–58, Jun. 2016.

[116] A. Q. Huang, "Medium-voltage solid-state transformer: Technology for a smarter and resilient grid," *IEEE Ind. Electron. Mag.*, vol. 10, no. 3, pp. 29–42, Sep. 2016.

[117] F. Briz, M. Lopez, A. Rodriguez, and M. Arias, "Modular power electronic transformers: Modular multilevel converter versus cascaded H-bridge solutions," *IEEE Ind. Electron. Mag.*, vol. 10, no. 4, pp. 6–19, Dec. 2016.

[118] R. Zhu and M. Liserre, "Grid-forming control of smart solid-state transformer in meshed network," in *Proc. IEEE 12th Int. Symp. Power Electron. Distrib. Gener. Syst.*, 2021, pp. 1–5.

[119] G. De Carne, G. Buticchi, M. Liserre, and C. Vournas, "Frequency-based overload control of smart transformers," in *Proc. IEEE Eindhoven PowerTech*, 2015, pp. 1–5.

[120] R. Zhu and M. Liserre, "Requirements for smart transformer," in *Proc. Int. Exhib. Conf. Power Electron. Intell. Motion Renewable Energy Energy Manage.*, 2019, pp. 7–9.

[121] G. De Carne, G. Buticchi, M. Liserre, P. Marinakis, and C. Vournas, "Coordinated frequency and voltage overload control of smart transformers," in *Proc. IEEE Eindhoven PowerTech*, 2015, pp. 1–5.

[122] S. Giacomuzzi, M. Langwasser, G. De Carne, G. Buja, and M. Liserre, "Smart transformer-based medium voltage grid support by means of active power control," *CES Trans. Elect. Mach. Syst.*, vol. 4, no. 4, pp. 285–294, Dec. 2020.

[123] L. Wang, Z. Qin, L. Beloqui Larumbe, and P. Bauer, "Python supervised co-simulation for A day-long harmonic evaluation of EV charging," *Chin. J. Elect. Eng.*, vol. 7, no. 4, pp. 15–24, 2021.

[124] J. E. Huber and J. W. Kolar, "Volume/weight/cost comparison of a 1 MVA 10 kV/400 V solid-state against a conventional low-frequency distribution transformer," in *Proc. IEEE Energy Convers. Congr. Expo.*, 2014, pp. 4545–4552.

[125] A. Borgaonkar, "Solid state transformers: A review of technology and applications," Indian Inst. Technol., New Delhi, India, Tech. Rep., Nov. 2015, doi: 10.13140/RG.2.1.1491.1443.

[126] J. Kolar and G. Ortiz, "Solid-State Transformers: Key components for future transportation and smart grid applications," 2014. Accessed: Jun. 13, 2022. [Online]. Available: https://www.pes-publications.ee.ethz.ch/uploads/tx_ethpublications/__PEAC_2014_finalfinal_041114.pdf

[127] A. Maitra, S. Rajagopalan, J.-S. Lai, M. DuVall, and M. McGranaghan, "Medium voltage stand alone DC fast charger," U. S. Patent Appl. 13/479 389, May 2013.

[128] J. S. Lai, W. H. Lai, S. R. Moon, L. Zhang, and A. Maitra, "A 15 kV class intelligent universal transformer for utility applications," in *Proc. IEEE Appl. Power Electron. Conf. Expo.*, 2016, pp. 1974–1981.

[129] S. Srdic, X. Liang, C. Zhang, W. Yu, and S. Lukic, "A SiC-based high performance medium-voltage fast charger for plug-in electric vehicles," in *Proc. IEEE Energy Convers. Congr. Expo.*, 2016, pp. 1–6.

[130] M. Vasiladiotis and A. Rufer, "A modular multiport power electronic transformer with integrated split battery energy storage for versatile ultrafast EV charging stations," *IEEE Trans. Ind. Electron.*, vol. 62, no. 5, pp. 3213–3222, May 2015.

[131] D. Sha, G. Xu, and Y. Xu, "Utility direct interfaced charger/discharger employing unified voltage balance control for cascaded H-bridge units and decentralized control for CF-DAB modules," *IEEE Trans. Ind. Electron.*, vol. 64, no. 10, pp. 7831–7841, Oct. 2017.

[132] C. Zhu *et al.*, "High-efficiency, medium-voltage-input, solid-state-transformer-based 400-kW/1000-V/400-A extreme fast charger for electric vehicles," Accessed: Jun. 13, 2022. [Online]. Available: https://www.energy.gov/sites/prod/files/2019/06/f64/elt241_zhu_2019_o_4.24_9.31pm_jl.pdf

[133] Z. Qin, Y. Tang, P. C. Loh, and F. Blaabjerg, "Benchmark of AC and DC active power decoupling circuits for second-order harmonic mitigation in kilowatt-scale single-phase inverters," *IEEE J. Emerg. Sel. Topics Power Electron.*, vol. 4, no. 1, pp. 15–25, Mar. 2016.

[134] J. W. Kolar and T. Friedli, "The essence of three-phase PFC rectifier systems—Part I," *IEEE Trans. Power Electron.*, vol. 28, no. 1, pp. 176–198, Jan. 2013.

[135] J. Kim, J. Lee, T. Eom, K. Bae, M. Shin, and C. Won, "Design and control method of 25 kW high efficient EV fast charger," in *Proc. 21st Int. Conf. Electric Mach. Syst.*, 2018, pp. 2603–2607.

[136] S. Chen, W. Yu, and D. Meyer, "Design and implementation of forced air-cooled, 140 kHz, 20 kW SiC MOSFET based Vienna PFC," in *Proc. IEEE Appl. Power Electron. Conf. Expo.*, 2019, pp. 1196–1203.

[137] J. A. Anderson, M. Haider, D. Bortis, J. W. Kolar, M. Kasper, and G. Deboy, "New synergetic control of a 20 kW isolated Vienna rectifier front-end EV battery charger," in *Proc. 20th Workshop Control Model. Power Electron.*, 2019, pp. 1–8.

[138] T. Nussbaumer, M. Baumann, and J. W. Kolar, "Comprehensive design of a three-phase three-switch buck-type PWM rectifier," *IEEE Trans. Power Electron.*, vol. 22, no. 2, pp. 551–562, Mar. 2007.

[139] A. Stupar, T. Friedli, J. Miniböck, and J. W. Kolar, "Towards a 99% efficient three-phase buck-type PFC rectifier for 400-V DC distribution systems," *IEEE Trans. Power Electron.*, vol. 27, no. 4, pp. 1732–1744, Apr. 2012.

[140] D. Aggeler *et al.*, "Ultra-fast DC-charge infrastructures for EVmobility and future smart grids," in *Proc. IEEE PES Innov. Smart Grid Technol. Conf. Eur.*, 2010, pp. 1–8.

[141] N. Celanovic and D. Boroyevich, "A comprehensive study of neutral-point voltage balancing problem in three-level neutral-point-clamped voltage source PWM inverters," *IEEE Trans. Power Electron.*, vol. 15, no. 2, pp. 242–249, Mar. 2000.

[142] S. Rivera, B. Wu, S. Kouro, V. Yaramasu, and J. Wang, "Electric vehicle charging station using a neutral point clamped converter with bipolar DC bus," *IEEE Trans. Ind. Electron.*, vol. 62, no. 4, pp. 1999–2009, Apr. 2015.

[143] L. Tan, B. Wu, V. Yaramasu, S. Rivera, and X. Guo, "Effective voltage balance control for bipolar-DC-bus-fed EV charging station with threelevel DC–DC fast charger," *IEEE Trans. Ind. Electron.*, vol. 63, no. 7, pp. 4031–4041, Jul. 2016.

[144] F. Briz, M. Lopez, A. Rodriguez, and M. Arias, "Modular power electronic transformers: Modular multilevel converter versus cascaded H-bridge solutions," *IEEE Ind. Electron. Mag.*, vol. 10, no. 4, pp. 6–19, Dec. 2016.

[145] R. T. Naayagi, A. J. Forsyth, and R. Shuttleworth, "High-power bidirectional DC-DC converter for aerospace applications," *IEEE Trans. Power Electron.*, vol. 27, no. 11, pp. 4366–4379, Nov. 2012.

[146] H. Qin and J. W. Kimball, "Solid-state transformer architecture usingACAC dual-active-bridge converter," *IEEE Trans. Ind. Electron.*, vol. 60, no. 9, pp. 3720–3730, Sep. 2013.

[147] A. Abu-Siada, J. Budiri, and A. Abdou, "Solid state transformers topologies, controllers, and applications: State-of-the-art literature review," *Electronics*, vol. 7, no. 11, Nov. 2018, Art. no. 298.

[148] H. Qin and J. Kimball, "AC-AC dual active bridge converter for solid state transformer," in *Proc. IEEE Energy Convers. Congr. Expo.*, 2009, pp. 3039–3044.

[149] M. Kang, P. Enjeti, and I. Pitel, "Analysis and design of electronic transformers for electric power distribution system," *IEEE Trans. Power Electron.*, vol. 14, no. 6, pp. 1133–1141, Nov. 1999.

[150] R. Bhaskar and V. Agarwal, "Dual pid loop controller for HF link inverter in two-stage SST," in *Proc. IEEE 7th Power India Int. Conf.*, 2016, pp. 1–4.

[151] H. Liu, K. Ma, Z. Qin, P. C. Loh, and F. Blaabjerg, "Lifetime estimation of MMC for offshore wind power HVDC application," *IEEE J. Emerg. Sel. Topics Power Electron.*, vol. 4, no. 2, pp. 504–511, Jun. 2016.

[152] H. Chen, A. Prasai, and D. Divan, "Dyna-C: A minimal topology for bidirectional solid-state transformers," *IEEE Trans. Power Electron.*, vol. 32, no. 2, pp. 995–1005, Feb. 2017.

[153] X. She, A. Q. Huang, and R. Burgos, "Review of solid-state transformer technologies and their application in power distribution systems," *IEEE J. Emerg. Sel. Topics Power Electron.*, vol. 1, no. 3, pp. 186–198, Sep. 2013.

[154] F. Zhang *et al.*, "Design and demonstration of a SiC-based 800-V/10-kV 1-MW solid-state transformer for grid-connected photovoltaic systems," in *Proc. IEEE 3rd Int. Future Energy Electron. Conf.*, 2017, pp. 1987–1990.

[155] J. A. Sabate, V. Vlatkovic, R. B. Ridley, and F. C. Lee, "Highvoltage, high-power, ZVS, full-bridge PWM converter employing an active snubber," in *Proc. 6th Annu. Appl. Power Electron. Conf. Exhib.*, 1991, pp. 158–163.

[156] J. G. Cho, J. W. Baek, C. Y. Jeong, and G.-H. Rim, "Novel zerovoltage and zero-current-switching full-bridge PWM converter using a simple auxiliary circuit," *IEEE Trans. Ind. Appl.*, vol. 35, no. 1, pp. 15–20, Jan. 1999.

[157] B. Yang, F. C. Lee, A. J. Zhang, and G. Huang, "LLC resonant converter for front end DC/DC conversion," in *Proc. 17th Annu. IEEE Appl. Power Electron. Conf. Expo.*, 2002, pp. 1108–1112.

[158] J. E. Huber, J. Miniböck, and J. W. Kolar, "Generic derivation of dynamic model for half-cycle DCM series resonant converters," *IEEE Trans. Power Electron.*, vol. 33, no. 1, pp. 4–7, Jan. 2018.

[159] M. Pahlevani, S. Pan, and P. Jain, "A hybrid phase-shift modulation technique for DC/DC converters with a wide range of operating conditions," *IEEE Trans. Ind. Electron.*, vol. 63, no. 12, pp. 7498–7510, Dec. 2016.

[160] Y. Nakakohara, H. Otake, T. M. Evans, T. Yoshida, M. Tsuruya, and K. Nakahara, "Three-phase LLC series resonant DC/DC converter using SiC MOSFETs to realize high-voltage and high-frequency operation," *IEEE Trans. Ind. Electron.*, vol. 63, no. 4, pp. 2103–2110, Apr. 2016.

[161] A. Coccia, F. Canales, P. Barbosa, and S. Ponnaluri, "Wide input voltage range compensation in DC/DC resonant architectures for onboard traction power supplies," in *Proc. Eur. Conf. Power Electron. Appl.*, 2007, pp. 1–10.

[162] H. M. Yoon, J. H. Kim, and E. H. Song, "Design of a novel 50 kW fast charger for electric vehicles," *J. Central South Univ.*, vol. 20, no. 2, pp. 372–377, Feb. 2013.

[163] H. Akagi, T. Yamagishi, N. M. L. Tan, S. Kinouchi, Y. Miyazaki, and M. Koyama, "Power-loss breakdown of a 750-V 100-kW 20-kHz bidirectional isolated DC–DC converter using SiC-MOSFET/SBD dual modules," *IEEE Trans. Ind. Appl.*, vol. 51, no. 1, pp. 420–428, Jan. 2015.

[164] J. E. Huber and J. W. Kolar, "Applicability of solid-state transformers in today's and future distribution grids," *IEEE Trans. Smart Grid*, vol. 10, no. 1, pp. 317–326, Jan. 2019.

[165] Z. Qin, Y. Shen, P. C. Loh, H. Wang, and F. Blaabjerg, "A dual active bridge converter with an extended high-efficiency range by DC blocking capacitor voltage control," *IEEE Trans. Power Electron.*, vol. 33, no. 7, pp. 5949–5966, Jul. 2018.

[166] Z. Qin, Z. Shen, F. Blaabjerg, and P. Bauer, "Transformer current ringing in dual active bridge converters," *IEEE Trans. Ind. Electron.*, vol. 68, no. 12, pp. 12 130–12 140, Dec. 2021.

[167] B. Zhao, Q. Song, W. Liu, and W. Sun, "Current-stress-optimized switching strategy of isolated bidirectional DC–DC converter with dual-phase-shift control," *IEEE Trans. Ind. Electron.*, vol. 60, no. 10, pp. 4458–4467, Oct. 2013.

[168] J. Huang, Y. Wang, Z. Li, and W. Lei, "Unified triple-phase-shift control to minimize current stress and achieve full soft-switching of isolated bidirectional DC-DC converter," *IEEE Trans. Ind. Electron.*, vol. 63, no. 7, pp. 4169–4179, Jul. 2016.

[169] Z. U. Zahid, Z. M. Dalala, R. Chen, B. Chen, and J.-S. Lai, "Design of bidirectional DC-DC resonant converter for vehicle-to-grid (V2G) applications," *IEEE Trans. Transp. Electrific.*, vol. 1, no. 3, pp. 232–244, Oct. 2015.

[170] J.-H. Jung, H.-S. Kim, M.-H. Ryu, and J.-W. Baek, "Design methodology of bidirectional CLLC resonant converter for high-frequency isolation of DC distribution systems," *IEEE Trans. Power Electron.*, vol. 28, no. 4, pp. 1741–1755, Apr. 2013.

[171] S. Zhao, Q. Li, F. C. Lee, and B. Li, "High-frequency transformer design for modular power conversion from medium-voltage AC to 400 VDC," *IEEE Trans. Power Electron.*, vol. 33, no. 9, pp. 7545–7557, Sep. 2018.

[172] Y. Shen, H. Wang, A. Al-Durra, Z. Qin, and F. Blaabjerg, "A bidirectional resonant DC–DC converter suitable for wide voltage gain range," *IEEE Trans. Power Electron.*, vol. 33, no. 4, pp. 2957–2975, Apr. 2018.

[173] L. Shu, W. Chen, and H. Jin, "A bidirectional three-phase triple-voltage LLC (T2-LLC) resonant converter for DC/DC stage in solid-state transformer and DC transformer applications," *IET Power Electron.*, vol. 15, pp. 434–446, Jan. 2022.

[174] C. Zhang, P. Li, Z. Kan, X. Chai, and X. Guo, "Integrated half-bridge CLLC bidirectional converter for energy storage systems," *IEEE Trans. Ind. Electron.*, vol. 65, no. 5, pp. 3879–3889, May 2018.

[175] D. Liu and H. Li, "Design and implementation of a DSP based digital controller for a dual half bridge isolated bi-directional DC-DC converter," in *Proc 21st Annu. IEEE Appl. Power Electron. Conf. Expo.*, 2006, pp. 695-699.

[176] M. Steiner and H. Reinold, "Medium frequency topology in railway applications," in *Proc. Eur. Conf. Power Electron. Appl.*, 2007, pp. 1–10.

[177] H. Hoffmann and B. Piepenbreier, "Medium frequency transformer for rail application using new materials," in *Proc. 1st Int. Electric Drives Prod. Conf.*, 2011, pp. 192–197.

[178] J. Huber, G. Ortiz, F. Krismer, N. Widmer, and J. W. Kolar, "$\eta - \rho$ Pareto optimization of bidirectional half-cycle discontinuous-conduction-mode series-resonant DC/DC converter with fixed voltage transfer ratio," in *Proc. 28th Annu. IEEE Appl. Power Electron. Conf. Expo.*, 2013, pp. 1413–1420.

[179] C. Zhao *et al.*, "Power electronic traction transformer'medium voltage prototype," *IEEE Trans. Ind. Electron.*, vol. 61, no. 7, pp. 3257–3268, Jul. 2014.

[180] K. Mainali, A. Tripathi, D. C. Patel, S. Bhattacharya, and T. Challita, "Design, measurement and equivalent circuit synthesis of high power HF transformer for three-phase composite dual active bridge topology," in *Proc. IEEE Appl. Power Electron. Conf. Expo.*, 2014, pp. 342–349.

[181] M. S. Agamy *et al.*, "A high power medium voltage resonant dual active bridge for MVDC ship power networks," *IEEE J. Emerg. Sel. Topics Power Electron.*, vol. 5, no. 1, pp. 88–99, Mar. 2017.

[182] Q. Chen, R. Raju, D. Dong, and M. Agamy, "High frequency transformer insulation in medium voltage SiC enabled air-cooled solid-state transformers," in *Proc. IEEE Energy Convers. Congr. Exp.*, 2018, pp. 2436–2443.

[183] D. Rothmund, T. Guillod, D. Bortis, and J. W. Kolar, "99% efficient 10 kV SiC-Based 7 kV/400 V DC transformer for future data centers," *IEEE Trans. Emerg. Sel. Topics Power Electron.*, vol. 7, no. 2, pp. 753–767, Jun. 2019.

[184] R. E. ON Energy Research Center, "Novel 5 MW DC converter put into operation," Accessed: Jun. 13, 2022. [Online]. Available: https://www.eonerc.rwth-aachen.de/go/id/dlnpc?lidx=1

[185] A. Reznik, M. G. Simões, A. Al-Durra, and S. M. Muyeen, "LCL filter design and performance analysis for grid-interconnected systems," *IEEE Trans. Ind. Appl.*, vol. 50, no. 2, pp. 1225–1232, Mar./Apr. 2014.

[186] M. H. Nehrir *et al.*, "A review of hybrid renewable/alternative energy systems for electric power generation: Configurations, control, and applications," *IEEE Trans. Sustain. Energy*, vol. 2, no. 4, pp. 392–403, Oct. 2011.

[187] J. Zhang, D. Guo, F. Wang, Y. Zuo, and H. Zhang, "Control strategy of interlinking converter in hybrid AC/DC microgrid," in *Proc. Int. Conf. Renewable Energy Res. Appl.*, 2013, pp. 97–102.

[188] J. Hu *et al.*, "A model predictive control strategy of PV-Battery microgrid under variable power generations and load conditions," *Appl. Energy*, vol. 221, pp. 195–203, Jul. 2018.

[189] B. Sun, T. Dragičević, F. D. Freijedo, J. C. Vasquez, and J. M. Guerrero, "A control algorithm for electric vehicle fast charging stations equipped with flywheel energy storage systems," *IEEE Trans. Power Electron.*, vol. 31, no. 9, pp. 6674–6685, Sep. 2016.

[190] P. Juan *et al.*, "Decentralized energy management strategy based on predictive controllers for a medium voltage direct current photovoltaic electric vehicle charging station," *Energy Convers. Manage.*, vol. 108, pp. 1–13, Jan. 2016.

[191] J. Zhu, Y. Liu, H. Lei, and T. Zhang, "A robust and model predictive control based energy management scheme for grid-connected microgrids," in *Proc. 2nd IEEE Conf. Energy Internet Energy Syst. Integration*, 2018, pp. 1–6.

[192] G. Haddadian, N. Khalili, M. Khodayar, and M. Shahidehpour, "Optimal scheduling of distributed battery storage for enhancing the security and the economics of electric power systems with emission constraints," *Electric Power Syst. Res.*, vol. 124, pp. 152–159, Jul. 2015.

[193] C. Jin, J. Tang, and P. Ghosh, "Optimizing electric vehicle charging with energy storage in the electricity market," *IEEE Trans. Smart Grid*, vol. 4, no. 1, pp. 311–320, Mar. 2013.

[194] P. M. Rocha Almeida, J. P. Iria, F. Soares, and J. A. P. Lopes, "Electric vehicles in automatic generation control for systems with large integration of renewables," in *Proc. IEEE Power Energy Soc. Gen. Meeting*, 2017, pp. 1–5.

[195] M. González Vayá and G. Andersson, "Self scheduling of plug-in electric vehicle aggregator to provide balancing services for wind power," *IEEE Trans. Sust. Energy*, vol. 7, no. 2, pp. 886–899, Apr. 2016.

[196] Q. Kang, J. Wang, M. Zhou, and A. C. Ammari, "Centralized charging strategy and scheduling algorithm for electric vehicles under a battery swapping scenario," *IEEE Trans. Intell. Transp. Syst.*, vol. 17, no. 3, pp. 659–669, Mar. 2016.

[197] E. Xydas, C. Marmaras, and L. M. Cipcigan, "A multi-agent based scheduling algorithm for adaptive electric vehicles charging," *Appl. Energy*, vol. 177, pp. 354–365, Sep. 2016.

ADNAN AHMAD (Student Member, IEEE) received the B.Sc. degree in electrical engineering from the University of Engineering and Technology, Peshawar, Pakistan, and the M.Sc. degree in electrical power and energy engineering from the COMSATS University of Information Technology, Islamabad, Pakistan, in 2010 and 2016, respectively. He is currently working toward the Ph.D. degree with the DC Systems, Energy Conversion, and Storage Group, Delft University of Technology, Delft, The Netherlands. From 2010 to 2011, he was a Trainee Engineer with MAN Diesel & Turbo, ATLAS Power Plant, Lahore, Pakistan. From 2012 to 2018, he was a Resident Engineer with the National Power and Control Center (NPCC), Islamabad, Pakistan, and worked in collaboration with Siemens and Alstom on the real-time data integration project of independent power producers with NPCC. From 2018 to 2020, he was an Electrical Engineer with Masaken Engineering Consultant, Fujairah, UAE. His research interests include power electronics converters, solid state transformers, renewable generation, energy storage systems, and ultra-fast charging stations.
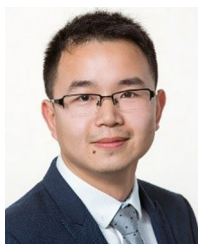
ZIAN QIN (Senior Member, IEEE) received the B.Eng. degree in automation from Beihang University, Beijing, China, in 2009, the M.Eng. degree in control science and engineering from the Beijing Institute of Technology, Beijing, China, in 2012, and the Ph.D. degree from Aalborg University, Aalborg, Denmark, in 2015. He is currently an Assistant Professor with the Delft University of Technology, Delft, The Netherlands. In 2014, he was a Visiting Scientist with Aachen University, Aachen, Germany. From 2015 to 2017, he was a Postdoctoral Research Fellow with Aalborg University. He has authored or coauthored more than 90 journals/conference papers, four book chapters, and two international patents in his research areas, which include power quality and stability of power electronics-based grid, solid state transformers. He has also worked on several European and Dutch national projects regarding the power quality of wind farms and EV charging. He is leading the research on solid-state transformers in FlexH2. He is an Associate Editor for IEEE TRANSACTIONS INDUSTRIAL ELECTRONICS, and a Guest Associate Editor of IEEE JOURNAL OF EMERGING AND SELECTED TOPICS and IEEE TRANSACTIONS ENERGY CONVERSION. He is a Distinguished Reviewer for 2020 of IEEE TRANSACTIONS OF INDUSTRIAL ELECTRONICS. He was the Technical Program Chair of IEEE-ISIE 2020, Technical Program Co-chair of IEEE-COMPEL 2020, Industrial Session Co-chair of ECCE-Asia 2020.

THIWANKA WIJEKOON (Senior Member, IEEE) received the B.Sc. degree (Hons.) in electrical and electronic engineering from the University of Peradeniya, Peradeniya, Sri Lanka, in 2001, and the Ph.D. degree in power electronics from the University of Nottingham, Nottingham, U.K., in 2006. Since 2016, he has been the Group Leader of the Power Electronics Technology R&D with Huawei's Nuremberg Research Center, Germany. He was a Lecturer in Electrical and Information Engineering at the University of Ruhuna, Sri Lanka, till 2003. From 2006 to 2010, he has been a Postdoctoral Research Fellow at the PEMC group, University of Nottingham working on multilevel power converters for more electric aircraft technology. In 2010, he joined GE Global Research-Europe as a Lead Research Engineer with High Power Electronics Lab, working on mega-watt power converters for MV applications. He holds more than 21 granted patents to date and 35 more patent applications pending and has coauthored more than 30 technical papers. His current research interests include power-electronic converter topologies, modulation, control and WBG based design of converter systems for applications in Solar PV, UPS, and EV.

PAVOL BAUER (Senior Member, IEEE) received the master's degree in electrical engineering from the Technical University of Kosice, Kosice, Slovakia, in 1985, and the Ph.D. degree from the Delft University of Technology, Delft, The Netherlands, in 1995. He is currently a Full Professor with the Department of Electrical Sustainable Energy, Delft University of Technology, and the Head of DC Systems, Energy Conversion and Storage Group. He is also an honorary Professor with Politehnica University Timisioira, Timisioira, Romania. From 2002 to 2003, he was working partially with KEMA (DNV GL, Arnhem) on different projects related to power electronics applications in power systems. He has authored or coauthored more than 110 journal and 450 conference papers in his research field (with H factor Google Scholar 52, Web of Science 41), he is the author or co-author of eight books, holds eight international patents and organized several tutorials at the international conferences. His main research interests include power electronics for charging of electric vehicles and DC grids. He has worked on many projects for industry concerning wind and wave energy, power electronic applications for power systems, such as smarttrafo, HVDC systems, projects for smart cities, such as PV charging of electric vehicles, PV and storage integration, contactless charging, and he participated in several Leonardo da Vinci, H2020, and Electric Mobility Europe EU projects as project partner (ELINA, INETELE, E-Pragmatic, Micact, Trolly 2.0, and OSCD), and the Co-ordinator of PEMCWebLab.com-Edipe, SustEner, and Eranet DCMICRO. He was the recipient of the title Prof. from the President of Czech Republic at the Brno University of Technology, Brno, Czechia, in 2008, and Delft University of Technology in 2016. He is the former Chairman of Benelux IEEE Joint Industry Applications Society, Power Electronics and Power Engineering Society Chapter, Chairman of the Power Electronics and Motion Control (PEMC) Council, Chairman of Benelux IEEE Industrial Electronics Chaper, Member of the Executive Committee of European Power Electronics Association (EPE), and also a Member of International Steering Committee at numerous conferences.